Development and Function of Smooth Muscle Cells is Modulated by *Hic1* in Mouse Testis

Aya Uchida[1,3], Sadman Sakib[1], Elodie Labit[1], Sepideh Abbasi[1], Wilder Scott[2], Michael Underhill[2], Jeff Biernaskie[1], Ina Dobrinski[1,*]

[1]*Department of Comparative Biology and Experimental Medicine, Faculty of Veterinary Medicine, University of Calgary, Calgary, Alberta, Canada*

[2]*The Biomedical Research Centre, University of British Columbia, Vancouver, British Columbia, Canada.*

[3]*Department of Veterinary Anatomy, The University of Tokyo, Bunkyo-ku, Tokyo, Japan.*

[*]Correspondence: idobrins@ucalgary.ca

Summary Statement: *Hypermethylated in cancer 1 (Hic1)* in testicular smooth muscle cells meditates the postnatal testicular development and secretion of fibronectin to modulate the testicular microenvironment.

ABSTRACT

In mammalian testis, contractile peritubular myoid cells (PMCs) regulate the transport of sperm and luminal fluid, while secreting growth factors and extra-cellular matrix (ECM) proteins to support the spermatogonial stem cell (SSC) niche. However, little is known about the role of testicular smooth muscle cells during the postnatal testicular development. Here we report age-dependent expression of *Hypermethylated in cancer 1* (*Hic1, ZBTB29*) in testicular smooth muscle cells, including PMCs and vascular smooth muscle cells in mouse. Postnatal deletion of *Hic1* in smooth muscle cells led to their increased proliferation and resulted in dilation of seminiferous tubules with increased numbers of PMC. These seminiferous tubules contained fewer Sertoli cells and more spermatogonia, and fibronectin was not detected in their basement membrane. The expression levels of genes encoding smooth muscle contractile proteins, *Acta2* and *Cnn1*, were down regulated in the smooth muscle cells lacking *Hic1*, and the seminiferous tubules appeared to have reduced contractility. These data imply a role for *Hic1* in determining the size of seminiferous tubules by regulating postnatal smooth muscle cell proliferation, subsequently affecting spermatogenesis at adulthood.

Keywords: *Hic1*, Peritubular myoid cell, Testicular smooth muscle cells, Mouse, Testis, Fibronectin

INTRODUCTION

Testicular smooth muscle cells, including peritubular myoid cells (PMCs) and vascular smooth muscle cells, are essential regulators of spermatogenesis in mammalian testis (Virtanen *et al.*, 1986). PMCs are myofibroblasts surrounding the surface area of seminiferous tubules (Fig. 1A), and their contractility helps propel the luminal fluid inside the seminiferous tubule towards the rete testis (Maekawa *et al.*, 1996). PMCs also secret extracellular matrix (ECM) proteins such as fibronectin, collagen IV and laminin to form the basement membrane that serves as an anchor to spermatogonia (Richardson *et al.*, 1995; Siu and Cheng, 2008). Blood vessels are on the surface of seminiferous tubules (Fig. 1A), to which undifferentiated spermatogonia have a biased distribution (Yoshida *et al.*, 2007). While it is traditionally well known that Sertoli cells support the spermatogonial stem cell (SSC) niche by secreting several growth factors (Meng *et al.*, 2000; Takashima *et al.*, 2015; Takase and Nusse, 2016), the importance of testicular smooth muscle cells in supporting the SSC niche is only beginning to be appreciated (Chen *et al.*, 2014; de Rooij, 2017). Testicular smooth muscle cells secret trophic factors such as glial cell line-derived neurotrophic factor (GDNF), colony stimulating factor 1 (CSF1) and chemokine (C-X-C motif) ligand 12 (CXCL12) to support the maintenance and self-renewal of SSCs (Oatley *et al.*, 2009; Chen *et al.*, 2016; Mayer *et al.*, 2018), while regulating the biosynthesis of retinoic acid (RA) to modulate the differentiation of SSCs (Davis and Ong, 1995). Testicular smooth muscle cells also modulate the function of Sertoli cells via hormonal (Welsh *et al*., 2009) and paracrine regulation (Verhoeven *et al*., 2000). During fetal testicular development, PMCs originate from the interstitial population of mesenchymal cells, and their postnatal fate is regulated by Sertoli cells (Rebourcet *et al.*, 2014). On the other hand, several studies have indicated PMCs as important regulators of Sertoli cells in prepubertal testicular development (Qian *et al*., 2013; Nurmio *et al*., 2012).

Kruppel/Zinc finger and BTB (POK/ZBTB) proteins are a family of transcription factors playing critical roles in development, cell differentiation and tumorigenesis in various organs (Kelly and Daniel, 2006; Lee and Maeda, 2012). In mammalian testis, *Zbtb16*, also known as promyelocytic leukemia zinc finger (PLZF), is expressed exclusively in undifferentiated spermatogonia, regulating their self-renewal to maintain the stem cell pool (Costoya *et al.*, 2004). Zbtb28, or Bcl6b, is known to regulate the self-renewal of SSCs in response to GDNF (Oatley *et al*., 2006). *Zbtb20* is expressed exclusively in Sertoli cells, yet its functional role is unclear (Jiang *et al.*, 2014). Although several members of the POK/ZBTB family serve as key regulators of cell differentiation and development, little is known about the expression patterns and functional roles of other POK/ZBTB proteins in mammalian testis.

In this study, we identified the age-dependent expression of one of the POK/ZBTB family members, *Hypermethylated in cancer 1 (HIC1, ZBTB29)* in testicular smooth muscle cells. *Hic1* is a zinc-finger transcriptional repressor first identified as a tumor suppressor gene (Zheng *et al.*, 2012). Homozygous disruption of *Hic1* results in embryonic and perinatal lethality due to developmental defects in various organs (Carter *et al*., 2000). This indicates the importance of *Hic1* in organ development, but also makes it difficult to analyze the functional roles of *Hic1* in adult tissue. By taking advantage of a 4-OHT-inducible Cre-loxP system, we ablated *Hic1* specifically in postnatal smooth muscle cells, which resulted in the increased proliferation of testicular smooth muscle cells during the early postnatal testicular development. This led to increased testicular size and enlargement of seminiferous tubules, which show reduced contractility and aberrant spermatogenesis. Mutant mice had increased numbers of PMCs, but fewer Sertoli cells. In addition, fibronectin, one of the ECM proteins constituting the basement membrane of the seminiferous tubules, was not detectable in the mutant PMCs. Taken together, this study revealed a novel role of *Hic1* in modulating the

proliferation of testicular smooth muscle cells, as well as shedding light on the importance of testicular smooth muscle cells in postnatal testicular development and spermatogenesis.

RESULTS

Hic1 expression in mouse testicular smooth muscle cells

To visualize *Hic1* expressing cells in mouse testis *in vivo*, we used *Hic1CreER^{T2}:ROSA26^{tdTomato}* mice, in which *Hic1* expressing cells can be visualized based on tdTomato upon 4-Hydroxytamoxifen (4-OHT) injections. To visualize *Hic1* expressing cells with tdTomato, *Hic1CreER^{T2}:ROSA26^{tdTomato}* mice were injected with tamoxifen 1 and 2 days before sampling (Fig. 1B). In 1wk-old *Hic1CreER^{T2}:ROSA26^{tdTomato}* mice injected with 4-OHT at P4 and P5 (n=3), we observed Hic1-tdTomato in a subset of the cells outlining the seminiferous tubules. To characterize the phenotype of Hic1-tdTomato^{+} cells, we performed immunostaining for alpha-smooth muscle actin (αSMA), which is a commonly used marker for smooth muscle cells (Skalli *et al.*, 1986). As a result, Hic1-tdTomato and αSMA immunoreactivity were co-localized (Fig. 1C,F,H), indicating that *Hic1* is expressed in the testicular smooth muscle cells. We further performed *in situ* hybridization in 1wk-old wild-type mice and validated *Hic1* expression in the testicular smooth muscle cells (Fig. 1D,E). Hic1-tdTomato was observed in peritubular myoid cells outlining the seminiferous tubule, as well as vascular smooth muscle cells distinguished by adjacent PECAM-1 expressing endothelial cells (Fig. 1C, F). Next, we investigated the proportion of *Hic1* expressing PMCs at each age. Although 56.18 ± 1.63 % of the PMCs were positive for Hic1-tdTomato at 1wk of age (n=4), the proportions of Hic1-tdTomato^{+} PMCs were lower, 2.95 ± 0.13 % in 4wk (n=4) and 1.76 ± 0.27 % in 8wk-old (n=4) mouse testis (Fig. 1G,H). Even if the labeling efficiency of *Hic1* expression with tdTomato was not high due to the low dose of tamoxifen used in this study (1mg tamoxifen/20g body weight), this result indicates that a limited

smooth muscle cell population expresses *Hic1* after postnatal testicular development. Since *Hic1* expression is induced by RA signaling in intestine (Burrows *et al.*, 2018), it might be possible that Hic1-tdTomato^{+} PMCs show biased expression to seminiferous epithelial stages IX–XII, where RA expression is high in adult mouse testis (Agrimson *et al.*, 2016). To see whether Hic1 expression in adult mouse testis is associated with specific seminiferous epithelial stage, we analyzed the epithelial stages of the seminiferous tubules with Hic1-tdTomato^{+} PMCs by using adult *Hic1CreER^{T2}:ROSA26^{tdTomato}* mice injected with 4-OHT 1 and 2 days before sampling (n=3). Hic1-tdTomato^{+} PMCs were present at frequencies of 51.1 (± 1.59) %, 25.1 (± 1.50) % and 23.7 (± 1.65) % in early (I-VI), mid (VII-VIII) and late (IX-XII) stages, respectively, which is similar to frequency of the seminiferous epithelial stages reported in (Oakberg, 1956): 46.86%, 19.96% and 33.16%. We next performed genetic linage tracing with *Hic1CreER^{T2}:ROSA26^{tdTomato}* mice, which were injected with 4-OHT at P4 and 5, to follow the fate of PMCs expressing *Hic1* at 1wk of age. The *Hic1* expressing cells at P4 and P5 labeled with tdTomato were traced up to 4wk-old (n=3) and adult (n=8) (Fig. 2A). As a result, 78.8 ± 1.43 % of PMCs in 4wk-old mice and 82.3 ± 5.77 % of PMCs in adult mice were observed to be tdTomato^{+} (Fig. 2B,C). The vascular smooth muscle cells adjacent to PECAM-1^{+} endothelial cells were also positive for Hic1-tdTomato after postnatal testicular development (Fig. 2D). These results suggest that the testicular smooth muscle cells in adult mouse testes, including PMCs and vascular smooth muscle cells, arise from *Hic1* expressing cells present at 1wk of age.

Increased testes size and dilation of seminiferous tubules in *Hic1* cKO mice

Having identified *Hic1* expression in the testicular smooth muscle cells and observed the expansion of *Hic1*$^{+}$ cells through testicular development, we then asked whether loss of *Hic1* expression in smooth muscle cells affects the postnatal testicular development and

consequent spermatogenesis. We used *aSMACreER^{T2}:Hic1^{flox}:ROSA26^{tdTomato}* mice to conditionally deplete *Hic1* in smooth muscle cells upon 4-OHT injection (Scott et al., 2019). In this study, all cKO, Het and WT littermates received 4-OHT at P4 and P5, and were analyzed at 1wk (WT: n=3 Het: n=3 cKO: n=3), 4wk (WT: n=14 Het: n=13 cKO: n=7), 8wk (WT: n=12 Het: n=11 cKO: n=9) and 6months-old (WT: n=1, cKO: n=1) (Fig. 3A). The proportion of testicular smooth muscle cells labelled with tdTomato in this mouse strain was 76.43 ± 1.49 % at 1wk of age (n=5). Interestingly, the testes of adult cKO mice were observed to be larger than the testes of WT mice, while 4wk-old mice did not exhibit an apparent difference in the size of testes (Fig. 3B). At 4wk-old, testis weight was 24.4 ± 4.9 mg in cKO, 25.1 ± 2.81 mg in Het and 24.0 ± 1.70 mg in WT, which were not significantly different from each other. However, at 8wk-old, testis weight was 105.4 ± 6.28 mg, which was significantly higher compared to 75.8 ± 3.10 mg in Het and 63.4 ± 2.67 mg in WT. When the testis weight (mg) was divided by body weight (g) in each animal to control for any effects of body weight on testis weight, relative testis weight (mg) / body weight (g) was similar in cKO: 1.55 ± 0.22, Het: 1.52 ± 0.12 and WT mice: 2.68 ± 0.09 at 4wk-old, but significantly higher in cKO: 3.79 ± 0.22 than in Het: 2.97 ± 0.11 and WT mice: 2.68 ± 0.15 at 8wk-old (Fig. 3C). To investigate the biological context underlying these larger and heavier testes in adult cKO mice, we first performed histological analysis at each age. While 1wk-old cKO mice did not exhibit any apparent phenotype (Fig. 3D), 4wk-old cKO mice had thin seminiferous tubules with relatively large lumen (Fig. 3D). At 8wk-old, seminiferous tubules of cKO mice were larger than in WT mice, with dilated lumen (Fig. 3D). This phenotype in 8wk-old cKO mice was also observed in 6 months-old mouse testis (Fig. 3D). The average area of cross-sectioned seminiferous tubule from 8wk-old cKO mice was significantly larger compared to WT mice (Fig. 3E). Although some of the vasculature also appeared to be dilated in cKO mice, it was not as clear as the seminiferous tubules due to the wide variety in

diameter of testicular blood vessels. In adult cKO mouse testis, we observed seminiferous tubules with very severe to relatively mild phenotypes of aberrant spermatogenesis within a single section (Fig. S1A). The proportion of degenerative seminiferous tubules, which are defined in this study as a cross-section of the seminiferous tubule that lacked one or more of the four germ cell layers such as seminiferous tubules shown in Fig.S1A'2–4, was significantly higher in cKO mice compared to WT mice (Fig. 3F). However, we observed sperm in the epididymis in cKO mice (Fig. S1B), suggesting that cKO mice retain the ability to undergo spermatogenesis and transport sperm into the epididymis. Accordingly, the weight of the seminal vesicles was 88.82 ± 15.74 mg in adult cKO mice (n=5) indicating physiological levels of circulating testosterone (Schlatt *et al.*, 2003). Sperm isolated from the epididymis in cKO mice had 56 ± 7.7 % motile sperm (n=5), comparable to sperm motility reported for tamoxifen-treated mice (dose: 0.6mg/kg, sperm motility rate: 61.8 ± 3.9%, Sadeghi *et al.*, 2019). Although seminiferous tubules in cKO mice were dilated, the rete testis region of cKO mice did not appear to be expanded (Fig. S1C). We also observed cell debris in the rete testis region in cKO mice (Fig. S1C), which may reflect the defects of spermatogenesis in cKO mice. Different from the cKO mice, estrogen receptor knock out (ERKO) mice have dilated seminiferous tubules and also expanded rete testis, which resulted from abnormal water reabsorption (Carreau and Hess, 2010; Hess *et al.*, 2018). The relative gene expression levels of *Esr1* and *Esr2* in sorted tdTomato^{+} smooth muscle cells from cKO mice were 1.35 ± 0.38 and 1.60 ± 0.53 respectively, not significantly different from WT mice (n=5 each, student's t-test). Therefore, we speculate that the dilated seminiferous tubules observed in this study are independent from regulation of luminal fluid through ERs.

Sertoli cells and germ cells are affected in *Hic1* cKO mice

Adult cKO mice had degenerative seminiferous tubules undergoing aberrant spermatogenesis. Since the functions of PMC can affect the distribution pattern and functions of Sertoli cells (Qian *et al.*, 2013), we performed immunostaining with an antibody against SOX9 as a marker for Sertoli cells (Hemendinger *et al.*, 2002). Although the seminiferous tubules of cKO mice were larger, $SOX9^+$ cells in the dilated seminiferous tubule were significantly fewer compared to WT mice (Fig. 4A,B). However, gene expression levels of functional markers of Sertoli cells, such as *Wilms' tumor 1 (wt1)*, *transferrin (trf1)*, *plasminogen activator (plat)*, *fatty acid binding protein 5 (fabp5)* and *reproductive homeobox 5 (rhox5)* were not significantly different between WT and cKO mice (Fig. S2A). Sertoli cells contribute to the blood-testis barrier (BTB) which prevents the infiltration of immune cells into the seminiferous tubules (Mruk and Cheng, 2015). To see the impact of cKO on Sertoli cell junctions, we next performed immunohistochemistry of Claudin11 and Occludin, which are tight junction proteins constituting BTB (Mazaud-Guittot *et al.*, 2010; McCabe *et al.*, 2016). Immunoreactive Claudin11 was observed in cKO mice around the $GATA4^+$ Sertoli cells (Fig. S2B), and immunoreactive Occludin was also present in cKO mice (Fig. S2C). Accordingly, junctional structures between Sertoli cells appeared intact in cKO mice when examined with electron microscopy (Fig. S2D). These results suggest that the functions of Sertoli cells and tight junctions between Sertoli cells were not disrupted, despite a lower number of Sertoli cells within the seminiferous tubules of cKO mice. Next, to investigate the impacts of *Hic1* cKO in smooth muscle cells on germ cells in more detail, we analyzed the distribution pattern of spermatogonia by performing immunohistochemistry for four different markers; GDNF family receptor alpha 1 (GFRα1), PLZF, LIN28A and c-KIT. GFRα1 is a marker for SSC-enriched subpopulations of undifferentiated spermatogonia (Hara *et al.*, 2014; Garbuzov et al., 2018), PLZF marks pan-undifferentiated spermatogonia (Buaas *et al.*,

2004; Costoya *et al.*, 2004), LIN28A marks a wide range of undifferentiated spermatogonia, including the early stage of differentiating spermatogonia (Zheng *et al.*, 2009; Chakraborty *et al.*, 2015) and c-KIT marks type A differentiating spermatogonia (Rossi *et al.*, 2000). As a result, GFRα1, PLZF, LIN28A and c-KIT$^+$ spermatogonia were observed in cKO mice similar to WT mice, even in the degenerated seminiferous tubules (Fig. 4C). We then quantified the number of cells positive for each marker per cross-sectioned seminiferous tubule and divided the number of undifferentiated spermatogonia by the number of Sertoli cells to reveal the "density" of spermatogonia for comparisons (Rebourcet *et al.*, 2017; Kitadate *et al.*, 2019). As a result, the densities of GFRα1, PLZF, LIN28A and c-KIT$^+$ germ cells were all significantly higher in cKO mice compared to WT mice (Fig. 4C,D). On the other hands, more differentiated germ cells such as spermatocytes positive for SCP3 (Yuan *et al.*, 2000) and late spermatids positive for HSP70 (Tsunekawa *et al.*, 1999) were significantly fewer in the cKO mice compared to WT mice (Fig. 4E,F). Next, we performed terminal deoxynucleotidyl transferase dUTP nick end labeling (TUNEL) analysis to compare the apoptotic incidence in VASA$^+$ germ cells and SOX9$^+$ Sertoli cells in the cKO and WT mice (Fig. 4G). The number of apoptotic cells per cross-sectioned seminiferous tubules was significantly larger in cKO mice compared to WT mice (Fig. 4G,H). We could not clarify which cell population specifically is undergoing cell death due to the lack of marker expressed by TUNEL-positive apoptotic cells (Fig. 4G). To analyze proliferation of germ cells in cKO mice, we performed immunohistochemistry for Cyclin D1 (CCND1) as a proliferation marker, which labels the G1-phase of the cell cycle (Ohta and Ichimura, 2001). The CCND1$^+$ cells observed in seminiferous tubule were not positive for GATA4, a marker for Sertoli cells (Fig. 4I). Hence, they are germ cells, specifically spermatogonia due to their location within the basal compartment of seminiferous epithelia. The numbers of CCND1$^+$ proliferative cells per cross-sectioned seminiferous tubule were not significantly different

from cKO and WT mice (Fig. 4J). Overall, these results imply a potential deficiency of germ cell differentiation from differentiating spermatogonia to spermatocyte, which might be a cause of increased apoptotic cells in the cKO seminiferous tubules.

Increased number of PMCs are covering the large seminiferous tubules in *Hic1* cKO mice

Noting the dilation of seminiferous tubules in cKO mice, we next asked how PMCs cover the increased surface area of the seminiferous tubules. To reveal the distribution pattern of PMCs, we performed immunochemistry against αSMA by using whole-mount samples of seminiferous tubules (Fig. 5A). As a result, the average surface area of individual PMCs was not significantly different in WT and cKO mice (Fig. 5B). We then quantified the number of PMCs per half circumference of the seminiferous tubule in each sample and discovered that there were more PMCs covering the surface area of the seminiferous tubule in cKO mice (Fig. 5C). The density of PMCs, which is represented as a number of PMCs in the 10000μm^2 of surface area in this study, was similar for each genotype (Fig. 5D). Taken together, increased surface area of cKO seminiferous tubules were covered by an increased number of PMCs, which have similar size and density to WT PMCs. Given the increased number of PMCs surrounding the seminiferous tubule in cKO mice, we next analyzed the proliferation of cKO smooth muscle cells at 1wk-old time point by performing Ki67 immunostaining. As a result, the proportion of testicular smooth muscle cells, including PMCs and vascular cells, positive for Ki67 was significantly higher in cKO mice compared to WT mice (Fig. 5E,F). We could not detect any PMCs positive for TUNEL in both WT and cKO mice at 1wk-old (data not shown). Occlusion or ligation of efferent ducts also cause the dilation of seminiferous tubules due to fluid accumulation, which eventually results in testicular atrophy (Hess *et al.*, 1991; Hess and Nakai, 2000). To test if the effect on PMC number observed in

the *Hic* cKO was secondary to fluid accumulation, we ligated the efferent ducts of wild-type mice. While this resulted in dilated rete testis and seminiferous tubules when efferent ducts where ligated at 7 wk of age, the number of PMCs per half circumference of seminiferous tubule was 8.64 ± 0.11 in control testis and 8.86 ± 0.11 in ligated testis, which was not significantly different (p=0.11, n=3, student's t-test). Although the number of PMCs was not affected, individual PMCs surrounding the dilated tubules in ligated testis appeared to be elongated to cover the increased surface area. Ligation at earlier time points did not result in fluid accumulation in the testis, thus did not cause the dilation of seminiferous tubules. Taken together, these results support the idea that the proliferation of prepubertal smooth muscle cells is promoted upon *Hic1* deletion, leading to the increased number of PMCs surrounding the enlarged seminiferous tubule in adult testis.

Impaired secretion of fibronectin from *Hic1* cKO PMCs

Importantly, PMCs secrete ECM proteins to contribute to the basement membrane of seminiferous tubules. Therefore, we examined the distribution of ECM proteins in the basement membrane in adult cKO mice by performing immunohistochemistry on collagen IV and LAMA1, one of the major laminin α chains in testis (Hager *et al.*, 2005) by using both paraffin sections (Fig. 6A) and cryosections (Fig. S3A,B). Strikingly, in cKO mice, hardly any immunoreactivity of fibronectin was observed around the seminiferous tubules (Figs 6A,S3A), in comparison with the signal in WT mice that appeared as a thick layer around the seminiferous tubules (Fig. 6A). In contrast, cKO mice appeared to have relatively strong signal of collagen IV and LAMA1 outlining the seminiferous tubule as a thicker layer (Figs 6A,S3A), while the immunoreactivity of collagen IV and LAMA1 in WT mice appeared as a thin layer around the seminiferous tubule (Figs 6A, S3A). In contrast to the PMCs, vasculature retained fibronectin expression in adult cKO mice (Fig. S3B). This might explain

why expression levels of *fn1* in the sorted tdTomato^{+} smooth muscle cells from adult WT and cKO mice, which include vascular smooth muscle cells and PMCs, were not different (Fig. S3C). We then observed the ultrastructure of PMCs from WT and cKO mice, respectively, by using electron microscopy. The cytoplasm of PMCs was sparse compared to WT mice (Figs 6B, S2D), and deposition of lipid-like structures (stars in Figs 6B,S2D) was frequently observed around the basement membrane of cKO mice.

Reduced expression of smooth muscle proteins in *Hic1* cKO mouse testis

From previous work, disruption of signaling in PMCs also resulted in the reduced expression of αSMA (Qian *et al.*, 2013). Therefore, we examined the expression of smooth muscle proteins; αSMA (*Acta2*) and Calponin 1 (*Cnn1*) (Walenta *et al.*, 2018). When we examined the expression level of each gene by using the whole testis, cKO mice showed significantly lower expression of both *Acta2* and *Cnn1* compared to WT mice (Fig. S3D). We further sorted the tdTomato^{+} testicular smooth muscle cells from adult WT and cKO mice to examine the expression levels of each gene exclusively in the smooth muscle cells in the absence of *Hic1*. As a result, tdTomato^{+} testicular smooth muscle cells from cKO mice showed reduced expression levels of both *Acta2* and *Cnn1* compared to WT mice (Fig. 6C). However, the relative expression levels of αSMA and CNN1 proteins in cKO mice were not significantly different from WT mice when quantified by Western blot using whole testis (αSMA: 1.12 ± 0.15, CNN1:1.05 ± 0.19, WT: n=5, cKO: n=4, student's t-test). This might be due to the different sensitivity of assays or the longevity or these proteins. Since αSMA and CNN1 regulate smooth muscle cell contraction (Winder and Walsh, 1993; Hinz *et al.*, 2001), we suspected reduced contractility of PMCs in the cKO seminiferous tubules. To assess the contractility of seminiferous tubules of WT and cKO mice, we performed time-course imaging analysis to observe the contractility of freshly isolated seminiferous tubules. As a

result, the seminiferous tubules from WT mice showed active contraction (Video. S1), while seminiferous tubules from adult cKO mice appeared to have less contractility compared to WT (Video. S2). Therefore, the contractility in cKO PMCs might be decreased due to reduced mRNA expression levels of smooth muscle proteins such as αSMA and CNN1.

DISCUSSSION

Hic1 may determine the size of seminiferous tubules by controlling the number of PMCs

The role of testicular smooth muscle cells in testicular development, SSC niche regulation and subsequently spermatogenesis are largely unknown. In this study, we demonstrate the expression of *Hic1* in testicular smooth muscle cells and describe that postnatal deletion of *Hic1* disrupted the development of seminiferous tubules and consequently spermatogenesis. *Hic1* is often found epigenetically silenced in various types of human cancers (Wales *et al.*, 1995; Chen *et al.*, 2003) and hence considered as a key player of cancer progression and proliferation (Zheng *et al.*, 2012). Consistent with a recent study demonstrating that the downregulation of *Hic1* promotes cell proliferation while overexpression of *Hic1* inhibited cell proliferation (Zhou *et al.*, 2019), *Hic1* deletion in smooth muscle cells in our study resulted in their increased proliferation, leading to the development of enlarged seminiferous tubules that were surrounded by a larger number of PMCs. In rodents, proliferation of PMCs and Sertoli cells ceases around 2 weeks of age, concomitantly with secretion of luminal fluid and entry into meiosis (Setchell 1970; Orth *et al.*, 1982; Rato *et al.*, 2010). Therefore, increased PMC proliferation at 1wk-old in this study was likely caused by the deletion of *Hic1*, as it precedes the increased luminal fluid content within the seminiferous tubules. Notably, tumor-suppressors such as Hippo and tuberous sclerosis tumor suppressor complex (TSC) are known to control organ size by regulating cell

growth (Pan *et al*. 2004; Sebio and Lenz, 2015). Although little is known about genes specifically regulating testis size, proliferation of PMCs contributes to the postnatal testicular growth (Nurmio *et al.*, 2012). Therefore, it might be possible that *Hic1* controls the size of seminiferous tubules by regulating proliferation of PMCs, which results in the appropriate size of seminiferous tubules to undergo healthy spermatogenesis. Although the majority of testicular smooth muscle cells in cKO mice were positive for tdTomato (Fig. S3A), a certain proportion of PMCs surrounding cKO seminiferous tubule were tdTomato-negative (Fig. 5A). Further study is required to clarify whether the increased proliferation of testicular smooth muscle cells was caused cell-autonomously or non-cell-autonomously by *Hic1* deletion.

Testicular smooth muscle cells may affect numbers of Sertoli cells and germ cells during postnatal testicular development

Here, we report a decreased number of Sertoli cells in cKO seminiferous tubules. While Sertoli cells regulate the number of germ cells and Leydig cells during testicular development (Rebourcet *et al.*, 2017; Heinrich *et al.*, 2020), a postnatal effect on PMC number has not been reported. Given that the proliferation of PMCs takes place earlier than Sertoli cells when induced by neonatal hemicastration or FSH administration (Nurmio *et al.*, 2012), and that Sertoli cell ablation in neonatal testis with benzalkonium chloride does not affect the number of PMCs *in vitro* (Yokonishi *et al*., 2020), it is possible that Sertoli cell number is affected by testicular smooth muscle cells in postnatal testicular development. Interestingly, while there were fewer Sertoli cells in cKO testes, the number of undifferentiated spermatogonia was increased. This may reflect a relative increase secondary to partial disruption or delay of meiotic differentiation of spermatogonia into spermatocytes. Similarly, mice fed with vitamin A-deficient diet, or treated with WIN18,446 to inhibit

retinaldehyde dehydrogenases have more spermatogonia due to meiotic inhibition (Endo *et al*., 2019). The increased number of spermatogonia in our study could also reflect the increased number of PMCs, as PMCs support spermatogonia both *in vivo* and *in vitro* (Chen *et al*., 2016). Despite the lower cell number, Sertoli cell functions and their support of spermatogonia did not appear to be disrupted in cKO mice, based on expression levels of genes related to Sertoli cell function and intact BTB components. However, fewer Sertoli cells could be a cause of reduced numbers of spermatocytes and spermatids, resulting in poor quality of spermatogenesis and reduced height of the seminiferous epithelium in cKO mice since meiosis is supported by Sertoli cells (Chen and Liu, 2015), and the number of spermatids correlates with Sertoli cell number (Orth *et al*., 1988).

Hic1 **as a potential modulator of fibronectin synthesis in PMCs**

Apart from its role in cell proliferation, *Hic1* modulates cell functions through its downstream signaling pathways (Chen *et al.*, 2005; Zhang *et al.*, 2007; Briones *et al.*, 2006). In this study, we reported the reduced expression of fibronectin in the PMCs lacking *Hic1*. Fibronectin is a glycoprotein which binds to β1 integrin and functions in cell adhesion, differentiation, and growth (Pankov and Yamada, 2002; Akiyama, 1996). In mammalian testis, both Sertoli cells and PMCs are known to participate in the production of basement membrane proteins (Hadley and Dym, 1987; Lian *et at.*, 1992; Kleinman *et al.*, 1993; Dym, 1994). Sertoli cells produce laminin and collagen IV but not fibronectin, while PMCs produce laminin, collagen IV and fibronectin (Richardson *et al*., 1995). Therefore, we assume that the biosynthesis of fibronectin is impaired in the *Hic1* depleted PMCs, which is potentially compensated by the secretion of other ECM proteins such as collagen IV and laminin. Notably, one of the receptors of fibronectin, β1-integrin, is expressed in spermatogonia (Schaller *et al*., 1993; Wennerberg *et al.*, 1996; Shinohara *et al*., 1999) and

may play a role in their differentiation (de Rooij *et al.,* 2008). In this study, we observed an increased number of undifferentiated spermatogonia and decreased population of differentiated germ cells later than spermatocyte in the cKO mice. Therefore, the deficiency of fibronectin in cKO mice might affect the capability of spermatogonia to differentiate by down-regulating their β1 integrin-associated signaling. Interestingly, *Hic1* is known to act as a modulator of Wnt/β-catenin signaling (Valenta *et al.,* 2006), and disrupted Wnt/β-catenin signaling in PMCs is reported to cause reduced expression of fibronectin (Qian *et al.,* 2013), while fibronectin is known as a direct target of Wnt/β-catenin signaling (Gradl *et al.*, 1999). Although we do not have direct evidence to show *Hic1* as a regulator of fibronectin in PMCs, it might be reasonable to speculate the low production of fibronectin in cKO mice in this study could be a result of aberrant Wnt/β-catenin signaling in PMCs, triggered by the lack of *Hic1*. Meanwhile, fibronectin was present in vasculature of adult cKO mice, but not in the basement membrane. This may reflect the distinct phenotype of PMCs and vascular smooth muscle cells, differentially affected by *Hic1* deletion. Expression levels of *fn1* in the sorted tdTomato^{+} cells from WT and cKO mice were not different. This might be explained in part by the high vasculature expression of *fn1*, whereas PMCs do not. However, we cannot exclude the possibility that the loss of fibronectin in cKO PMCs could be secondary to the enlargement of cKO seminiferous tubules. Since tdTomato^{+} cells sorted from *aSMACreER^{T2}:ROSA^{tdTomato}:Hic1^{flox}* mice include both PMCs and vascular smooth muscle cell populations, this was a technical limitation to distinguish these two smooth muscle cell populations. It remains a challenge to study the function of PMCs and vascular smooth muscle cells separately due to the lack of cell type specific markers allowing isolation of pure populations.

Contractility of PMCs and the size of the lumen of seminiferous tubules

Contractility of vascular smooth muscle cells regulates the size of lumen inside the blood vessels (Brozovich *et al.*, 2016), while airway smooth muscle cells in the lung designate the diameter of airway lumen (Amrani and Panettieri, 2003). Thus, we suspect that the dilated lumen of seminiferous tubules observed in this study is partly due to the reduced contractility of PMCs (see Supplementary videos 1–2). β1 integrin is the most predominant integrin expressed in the vascular smooth muscle cells (Hillis *et al.*,1998; Turlo *et al.*, 2014), and adhesion of smooth muscle cells to fibronectin is known to coordinate the cell contraction of smooth muscle cells (Hong *et al.*, 2012). Considering the reduced production of fibronectin observed in this study, contractility of cKO smooth muscle cells might be affected cell-autonomously due to their reduced biosynthesis of fibronectin caused by *Hic1* deficiency. In the *Hic1* depleted smooth muscle cells, expression levels of genes associated with smooth muscle cell contraction such as *Acta2* and *Cnn1* were significantly decreased in cKO mouse testis (Figs 6C,S3D). Since *Acta2* upregulates cell contractility (Hinz *et al.*, 2001) and *Cnn1* regulates smooth muscle cell contraction (Winder and Walsh, 1993), it is highly probable that the contractility of cKO PMCs is impaired. Interestingly, disruption of Wnt/β-catenin signaling in PMCs is reported to also cause reduced immunoreactivity of αSMA (Qian *et al.*, 2013). On the other hand, androgen action via androgen receptor (AR) in PMCs is crucial for spermatogenesis and male fertility (Welsh *et al*., 2009, 2010; Chen *et al*., 2014), and upregulation of AR causes increased protein expression of both CNN1 and αSMA in PMCs (Mayer *et al.*, 2018). Therefore, the reduced mRNA expression levels of *Acta2* and *Cnn1* in smooth muscle cells in this study could also be explained if Wnt/β-catenin signaling and/or AR signaling is affected by the deletion of *Hic1*.

In conclusion, our results demonstrate an important role of *Hic1* in testicular smooth muscle cells to modulate their proliferation, affecting the size of seminiferous tubules and subsequent spermatogenesis. Our findings highlight a novel function of testicular smooth muscle cells in postnatal testicular development.

MATERIALS AND METHODS

Animals

Hic1CreER^{T2}:ROSA26^{tdTomato} mice (Scott *et al.*, 2019) and *aSMACreER^{T2}:ROSA26^{tdTomato}* mice (Shin *et al.*, 2020) were used in this study. *aSMACreER^{T2}:ROSA26^{tdTomato}* mice were then crossed with *Hic1$^{flox/flox}$* mice (Burrows *et al.*, 2018) to generate *aSMACreER^{T2}: Hic1$^{flox/+}$:ROSA26^{tdTomato}* mice. *aSMACreER^{T2}: Hic1$^{flox/+}$:ROSA26^{tdTomato}* mice were then mated each other to generate *aSMACreER^{T2}: Hic1$^{+/+}$:ROSA26^{tdTomato}* (WT), *aSMACreER^{T2}: Hic1$^{flox/+}$:ROSA26^{tdTomato}* (Het) and *aSMACreER^{T2}: Hic1$^{flox/flox}$:ROSA26^{tdTomato}* (cKO) littermates. Tamoxifen (4-OHT; Sigma) was dissolved in 100% ethanol (1mg/30µl), diluted into corn oil and then injected intraperitoneally to mice (1mg 4-OHT /20g body weight). All animal experiments were approved by the University of Calgary Health Sciences Animal Care Committee and were in accordance with guidelines by the Canadian Council on Animal Care. Experiments of efferent duct ligation were performed by using 7wk-old ICR mice (SLC Inc.) in accordance with the Guidelines for Animal Use and Experimentation of the University of Tokyo.

Histology and Immunohistochemistry

Testes were fixed in 4% paraformaldehyde (PFA) or Bouin's solution at 4°C overnight, dehydrated in a series of ethanol and embedded in paraffin. For cryo-blocks, testes

were fixed for 1 hour in 4% PFA at room temperature, followed by 30 minutes in 10% sucrose and 30 minutes in 20% sucrose, and then subsequently snap frozen in OCT compound (Leica). For hematoxylin and eosin (HE) staining, paraffin sections were immersed in Mayer's Hematoxylin Solution (Sigma) for 3.5 minutes and in Eosin Alcohol Solution for 30 seconds at room temperature. For immunohistochemistry, paraffin sections and cryo-sections (both 5μm in thickness) were incubated overnight at 4°C with the antibodies listed in Table S1. For whole-mount analysis, testes were fixed in 4% PFA at 4°C overnight, removed from tunica albuginea, and dispersed in cold phosphate-buffered saline (PBS). Seminiferous tubule fragments were isolated manually, permeabilized with a gradient series of methanol, and incubated overnight at 4°C with anti-αSMA (1:200 dilution; Sigma) antibody. TUNEL assay was performed by using the DeadEnd^{TM} Fluorometric 488 system (Promega) according to manufacturer's instructions. Immunoreactions were visualized by using Alexafluor-488/555/594/680 conjugated secondary antibodies (Abcam) or biotin-conjugated secondary antibodies with the Elite ABC Kit (Vector Laboratories). Samples were analyzed by fluorescence microscopy (Zeiss imager M2) or Leica TCS SP8 confocal laser microscopy. To ensure reproducibility of results, testes from at least three animals at each age were used, and sections from WT, Het and cKO littermates were processed in parallel.

Cell counting and seminiferous epithelia staging

More than 50 cross-sectioned seminiferous tubules were analyzed per sample for quantitative analysis using paraffin sections, and more than 30 seminiferous tubules were analyzed per sample for the quantification using whole-mount samples. To examine the density of PMCs, the number of PMCs in the surface area of 10000μm^2 was counted for each whole-mount seminiferous tubule. To quantify the proportion of tdTomato$^+$ PMCs, more than

500 cells per sample were counted. To quantify the proportion of $Ki67^+$ cells, more than 200 smooth muscle cells per sample were counted, including PMCs and vascular cells. To assess the relative germ cell density, the number of germ cells was divided by the number of Sertoli cells in the same section as previously reported (Kitadate *et al.*, 2019). The areas of more than 50 PMCs and cross-sectioned seminiferous tubules were measured using the Image J software (NIH) for quantification. The seminiferous epithelial stages were classified into early (I-VI), mid (VII-VIII) and late (IX-XII) stages, based on the association of the cells within the seminiferous epithelia (Meistrich and Hess, 2013). Briefly, seminiferous epithelia containing both round spermatids and elongated spermatids were categorized at early stage, unless preleptotene spermatocytes were observed together with elongated spermatids aligned at the lumen of seminiferous tubule (mid stage). Seminiferous tubules lacking round spermatids were categorized as late stage.

Electron microscopy

Tissue was trimmed and fixed in 2.5% glutaraldehyde in 0.1M sodium cacodylate buffer (pH 7.4) overnight, and post-fixed with 1% osmium in veronal-acetate buffer. Tissues were then stained in block overnight with 0.5% uranyl acetate in veronal-acetate buffer (pH 6.0), dehydrated and embedded in Spurr's resin. Sections were cut on a Leica Ultracut UCT microtome with a Diatome diamond knife at a thickness setting of 50 nm and then stained with uranyl acetate and lead citrate. The sections were analyzed using Hitach H-7650 TEM at 120KV.

RNA *in situ* hybridization

Testes were fixed in 10% neutral buffer formalin at room temperature overnight, dehydrated in a series of ethanol and embedded in paraffin. Paraffin-embedded sections (5μm

in thickness) were processed for RNA *in situ* detection using RNAscope® 2.5 HD Assay Red Manual with RNAscope® probe-Mm *Hic1* (ACDBio) according to the manufacturer's instructions. Some of the stained sections were subsequently subjected to αSMA immunohistochemistry with the Elite ABC Kit (Vector Laboratories).

Cell sorting

Testes from adult *aSMACreER^{T2}:ROSA^{tdTomato}:Hic1$^{+/+}$* (WT) and *Hic1$^{flox/flox}$* (cKO) mice injected with 4-OHT at P4 and P5 were dissociated to single cells and sorted on a FACSAria III (Becton Dickinson) for smooth muscle cells characterized as the tdTomato^{+} cell population.

RNA isolation and real-time qPCR

RNA was isolated from testis tissue by using RNeasy Mini Kit (Qiagen) followed by reverse transcription using ABI High Capacity cDNA synthesis kit according to manufacturer's instructions. For the sorted cells (<100,000 cells), RNA was isolated by using Pico Pure™ RNA Isolation Kit (Applied Biosystems) followed by reverse transcription using the Super Script™ IV VILO™ Master Mix (Thermo Fisher). Quantitative real-time PCR was performed using ABI 7500 Fast PCR (ABI) in SYBR Green system by using the primers listed in Table S2, and in TaqMan® system (Applied Biosystems) by using the probes for *Hic1* (Mm03058120_m1) and *HPRT* (Mm03024075_m1). The expression levels of each gene were presented relative to *HPRT* expression.

Western blot

Western blot was performed as reported previously (Valenzuela-Leon and Dobrinski, 2017). See supplementary Materials and Methods for further details.

Efferent duct ligation

The efferent duct of 7wk-old wild-type mouse testis was ligated under a dissecting microscope as reported previously (Smith, 1962). Samples were collected 1 week after the ligation and subjected to analysis. See supplementary Materials and Methods for further details.

Sperm motility evaluation

Epididymides collected from adult cKO mice were placed in a 300μL droplet of warm (37°C) PBS, finely minced with scissors and kept at 37°C for 15 min to allow sperm to swim out. 3μL of the aliquot was then subjected to computerized sperm analysis (CASA) system (Spermvision® Version 3.5.6.2, Minitube, Verona, WI, USA), in which seven fields were evaluated per sample. Seminal vesicles from adult cKO mice were collected and weighted as reported previously (Schlatt et al., 2003).

Time-course analysis of the tubule contraction

Seminiferous tubules were freshly isolated from adult cKO mice and wild-type mice and placed onto the slides in DMEM with 10% FBS. The images of the seminiferous tubule were taken every 10 seconds for 5 min by using the microscope (Zeiss imager M2).

Statistical Analysis

Quantitative data are represented as mean ± SEM. Data were analyzed using R (version 3.6.1). Student's t-test was performed for single comparisons between two groups. For more than two groups, data were analyzed by one-way ANOVA with Tukey's multiple comparison test. Box plots in this study were generated using R software, applying the R package of ggpubr. The median is shown as a line in the center of the box, and the whiskers

show the range of sample distribution, excluding outliers. $P < 0.05$ was considered significant, and the levels of significance are represented as *P<0.05, **P<0.01, ***P<0.005 and ****P<0.001.

Acknowledgement

Authors thank members of the I.D. and J.B. laboratories, especially L.Sue for her excellent technical support and A. Bondareva and R.Dardari for their management and support. We also thank Y.Kanai, R.Hiramatsu and his laboratory at the University of Tokyo for their advice and supports.

Competing Interests

The authors have declared that no competing interests exist.

Funding

This study was supported by NIH/ORIP (9 R01 OD016575 to I.D.), Canadian Institutes of Health Research (Project grant #156444 to J.B.) and Ito Foundation for International Education Exchange (to A.U.). A. U is a research fellow of Japan Society for the Promotion of Science.

Data Availability

The authors confirm that all data underlying the findings are fully available without restriction. All relevant data are within the paper and its Supporting Information files.

REFERENCES

Agrimson, K. S., Onken, J., Mitchell, D., Topping, T. B., Chiarini-Garcia, H., Hogarth, C. A. and Griswold, M.D. (2016). Characterizing the spermatogonial response to retinoic acid during the onset of spermatogenesis and following synchronization in the neonatal mouse testis. *Biol. Reprod.* **95**, 81.

Akiyama, S. K. (1996). Integrins in cell adhesion and signaling. *Hum. Cell* **9**, 181-186.

Amrani, Y. and Panettieri, R. A. (2003). Airway smooth muscle: Contraction and beyond. *Int. J. Biochem. Cell. Biol.* **35**, 272-276.

Briones, V. R., Chen, S., Riegel, A. T. and Lechleider, R. J. (2006). Mechanism of fibroblast growth factor-binding protein 1 repression by TGF-beta. *Biochem. Biophys. Res. Commun.* **345**, 595-601.

Brozovich, F. V., Nicholson, C. J., Degen, C. V., Gao, Y. Z., Aggarwal, M. and Morgan, K. G. (2016). Mechanisms of vascular smooth muscle contraction and the basis for pharmacologic treatment of smooth muscle disorders. *Pharmacol. Rev.* ***68***, 476-532.

Buaas, F. W., Kirsh, A. L., Sharma, M., McLean, D. J., Morris, J. L., Griswold, M. D., de Rooij, D.G. and Braun, R.E. (2004). Plzf is required in adult male germ cells for stem cell self-renewal. *Nat. Genet.* **36**, 647-652.

Burrows, K., Antignano, F., Chenery, A., Bramhall, M., Korinek, V., Underhill, T. M. and Zaph, C. (2018). HIC1 links retinoic acid signalling to group 3 innate lymphoid cell-dependent regulation of intestinal immunity and homeostasis. *PLoS Pathog.* **14**, e1006869.

Carreau, S. and Hess, R. A. (2010). Oestrogens and spermatogenesis. *Trans. R. Soc. B.* **365**, 1517-1535.

Carter, M. G., Johns, M. A., Zeng, X., Zhou, L., Zink, M. C., Mankowski, J. L., Donovan, D.M. and Baylin, S.B. (2000). Mice deficient in the candidate tumor suppressor gene Hic1 exhibit developmental defects of structures affected in the miller-dieker syndrome. *Hum. Mol. Gen.* **9**, 413-419.

Chakraborty, P., Buaas, F. W., Sharma, M., Snyder, E., de Rooij, D. G. and Braun, R. E. (2014). LIN28A marks the spermatogonial progenitor population and regulates its cyclic expansion. *Stem Cells,* **32,** 860-873.

Chen, L. Y., Brown, P. R., Willis, W. B. and Eddy, E. M. (2014). Peritubular myoid cells participate in male mouse spermatogonial stem cell maintenance. *Endocrinology*, **155**, 4964-4974.

Chen, L. Y., Willis, W. D. and Eddy, E. M. (2016). Targeting the gdnf gene in peritubular myoid cells disrupts undifferentiated spermatogonial cell development. *Proc. Natl. Acad. Sci. U. S. A.* **113**, 1829-1834.

Chen, S.R. and Liu, Y.X. (2015). Regulation of spermatogonial stem cell self-renewal and spermatocyte meiosis by Sertoli cell signaling. *Reproduction* **149**, R159-67.

Chen, W. Y., Wang, D. H., Yen, R. C., Luo, J., Gu, W. and Baylin, S. B. (2005). Tumor suppressor HIC1 directly regulates SIRT1 to modulate p53-dependent DNA-damage responses. *Cell* **123**, 437-448.

Chen, W. Y., Zeng, X., Carter, M. G., Morrell, C. N., Chiu Yen, R. W., Esteller, M., Watkins, D.N., Herman, J.G., Mankowski, J.L. and Baylin, S.B. (2003). Heterozygous disruption of Hic1 predisposes mice to a gender-dependent spectrum of malignant tumors. *Nat. Genet.* **33**, 197-202.

Costoya, J. A., Hobbs, R. M., Barna, M., Cattoretti, G., Manova, K., Sukhwani, M., Orwig, K.E., Wolgemuth, D.J. and Pandolfi, P.P. (2004). Essential role of plzf in maintenance of spermatogonial stem cells. *Nat. Genet.* **36**, 653-659.

Davis, J. T. and Ong, D. E. (1995). Retinol processing by the peritubular cell from rat testis. *Biol. Reprod.* **52**, 356-364.

de Rooij, D. G. (2017). The nature and dynamics of spermatogonial stem cells. *Development* **144**, 3022-3030.

de Rooij, D. G., Repping, S. and van Pelt, A. M. (2008). Role for adhesion molecules in the spermatogonial stem cell niche. *Cell Stem Cell* **3**, 467-468.

Dym, M. (1994). Basement membrane regulation of sertoli cells. *Endocr. Rev.* **15**, 102-115.

Endo, T., Mikedis, M.M., Nicholls, P.K., Page, D.C. and de Rooij, D.G. (2019). Retinoic Acid and Germ Cell Development in the Ovary and Testis. *Biomolecules* **9**, 10.3390.

Garbuzov, A., Pech, M. F., Hasegawa, K., Sukhwani, M., Zhang, R. J., Orwig, K. E. and Artandi, S.E. (2018). Purification of GFRalpha1+ and GFRalpha1- spermatogonial stem cells reveals a niche-dependent mechanism for fate determination. *Stem Cell Rep.* **10**, 553-567.

Gradl, D., Kuhl, M. and Wedlich, D. (1999). The Wnt/Wg signal transducer beta-catenin controls fibronectin expression. *Mol. Cell. Biol.* **19,** 5576-5587.

Grasso, M., Fuso, A., Dovere, L., de Rooij, D. G., Stefanini, M., Boitani, C. and Vicini, E. (2012). Distribution of GFRA1-expressing spermatogonia in adult mouse testis. *Reproduction* **143**, 325-332.

Hadley, M. A. and Dym, M. (1987). Immunocytochemistry of extracellular matrix in the lamina propria of the rat testis: Electron microscopic localization. *Biol. Reprod.* **37**, 1283-1289.

Hager, M., Gawlik, K., Nystrom, A., Sasaki, T. and Durbeej, M. (2005). Laminin {alpha}1 chain corrects male infertility caused by absence of laminin {alpha}2 chain. *Am. J. Pathol.* **167**, 823-833.

Hara, K., Nakagawa, T., Enomoto, H., Suzuki, M., Yamamoto, M., Simons, B. D. and Yoshida, S. (2014). Mouse spermatogenic stem cells continually interconvert between equipotent singly isolated and syncytial states. *Cell Stem Cell* **14**, 658-672.

Heinrich, A., Potter, S.J., Guo, L., Ratner, N. and DeFalco, T. (2020). Distinct Roles for Rac1 in Sertoli Cell Function during Testicular Development and Spermatogenesis. *Cell Rep.* **31**, 107513.

Hemendinger, R. A., Gores, P., Blacksten, L., Harley, V. and Halberstadt, C. (2002). Identification of a specific sertoli cell marker, Sox9, for use in transplantation. *Cell Transplant.* **11**, 499-505.

Hess, R. A. and Cooke, P. S. (2018). Estrogen in the male: A historical perspective. *Biol. Reprod.* **99**, 27-44.

Hess, R. A., Moore, B. J., Forrer, J., Linder, R. E. and Abuel-Atta, A. A. (1991). The fungicide benomyl (methyl 1-(butylcarbamoyl)-2-benzimidazolecarbamate) causes testicular dysfunction by inducing the sloughing of germ cells and occlusion of efferent ductules. *Toxicol. Sci.* **17**, 733-745.

Hess, R. A. and Nakai, M. (2000). Histopathology of the male reproductive system induced by the fungicide benomyl. *Histol. Histopathol.* **15**, 207-224.

Hillis, G. S., Mlynski, R. A., Simpson, J. G. and MacLeod, A. M. (1998). The expression of beta 1 integrins in human coronary artery. *Basic Res. Cardiol.* **93**, 295-302.

Hinz, B., Celetta, G., Tomasek, J. J., Gabbiani, G. and Chaponnier, C. (2001). Alpha-smooth muscle actin expression upregulates fibroblast contractile activity. *Mol. Biol. Cell* **12**, 2730-2741.

Hong, Z., Sun, Z., Li, Z., Mesquitta, W. T., Trzeciakowski, J. P. and Meininger, G. A. (2012). Coordination of fibronectin adhesion with contraction and relaxation in microvascular smooth muscle. *Cardiovasc. Res.* **96**, 73-80.

Jiang, X., Zhang, H., Yin, S., Zhang, Y., Yang, W., Zheng, W., Wang, L., Wang, Z., Bukhari, I., Cooke, H.J., *et al.* (2014). Specific deficiency of plzf paralog, Zbtb20, in sertoli cells does not affect spermatogenesis and fertility in mice. *Sci. Rep.* **4**, 7062.

Kelly, K. F. and Daniel, J. M. (2006). POZ for effect--POZ-ZF transcription factors in cancer and development. *Trends Cell Biol.* **16**, 578-587.

Kitadate, Y., Jorg, D. J., Tokue, M., Maruyama, A., Ichikawa, R., Tsuchiya, S., Segi-Nishida, E., Nakagawa, T., Uchida, A., Kimura-Yoshida, C., *et al.* (2019). Competition for mitogens regulates spermatogenic stem cell homeostasis in an open niche. *Cell Stem Cell* **24**, 79-92.

Kleinman, H. K., Weeks, B. S., Schnaper, H. W., Kibbey, M. C., Yamamura, K. and Grant, D. S. (1993). The laminins: A family of basement membrane glycoproteins important in cell differentiation and tumor metastases. *Vitam. Horm.* **47**, 161-186.

Lee, S. U. and Maeda, T. (2012). POK/ZBTB proteins: An emerging family of proteins that regulate lymphoid development and function. *Immunol. Rev.* **247**, 107-119.

Lian, G., Miller, K. A. and Enders, G. C. (1992). Localization and synthesis of entactin in seminiferous tubules of the mouse. *Biol. Reprod.* **47**, 316-325.

Maekawa, M., Kamimura, K. and Nagano, T. (1996). Peritubular myoid cells in the testis: Their structure and function. *Arch. Histol. Cytol.* **59**, 1-13.

Mayer, C., Adam, M., Walenta, L., Schmid, N., Heikela, H., Schubert, K., Flenkenthaler, F., Dietrich, K.G., Gruschka, S., Arnold, G.J., *et al.* (2018). Insights into the role of androgen receptor in human testicular peritubular cells. *Andrology* **6**, 756-765.

Mazaud-Guittot, S., Meugnier, E., Pesenti, S., Wu, X., Vidal, H., Gow, A. and Le Magueresse-Battistoni, B. (2010). Claudin 11 deficiency in mice results in loss of the Sertoli cell epithelial phenotype in the testis. *Biol. Reprod.* **82**, 202-213.

McCabe, M.J., Foo, C.F., Dinger, M.E., Smooker, P.M. and Stanton, P.G. (2016). Claudin-11 and occludin are major contributors to Sertoli cell tight junction function, in vitro. *Asian J. Androl.* **18**, no. 4, pp. 620-626.

Meistrich, M.L. and Hess, R.A. (2013). Assessment of spermatogenesis through staging of seminiferous tubules. *Methods Mol. Biol.* **927**, 299-307.

Meng, X., Lindahl, M., Hyvonen, M. E., Parvinen, M., de Rooij, D. G., Hess, M. W., Raatikainen-Ahokas, A., Sainio, K., Rauvala, H., Lakso, M., *et al.* (2000). Regulation of cell fate decision of undifferentiated spermatogonia by GDNF. *Science* **287**, 1489-1493.

Mruk, D.D. and Cheng, C.Y. (2015). The Mammalian Blood-Testis Barrier: Its Biology and Regulation. *Endocr. Rev.* **36**, 564-591.

Nurmio, M., Kallio, J., Adam, M., Mayerhofer, A., Toppari, J. and Jahnukainen, K. (2012). Peritubular myoid cells have a role in postnatal testicular growth. *Spermatogenesis* **2**, 79-87.

Oakberg, E. F. (1956). Duration of spermatogenesis in the mouse and timing of stages of the cycle of the seminiferous epithelium. *Am. J. Anat.* **99**, 507-516.

Oatley, J. M., Avarbock, M. R., Telaranta, A. I., Fearon, D. T. and Brinster, R. L. (2006). Identifying genes important for spermatogonial stem cell self-renewal and survival. *Proc. Natl. Acad. Sci. U. S. A.* **103**, 9524-9529.

Oatley, J. M. and Brinster, R. L. (2012). The germline stem cell niche unit in mammalian testes. *Physiol. Rev.* **92**, 577-595.

Oatley, J. M., Oatley, M. J., Avarbock, M. R., Tobias, J. W. and Brinster, R. L. (2009). Colony stimulating factor 1 is an extrinsic stimulator of mouse spermatogonial stem cell self-renewal. *Development* **136**, 1191-1199.

Ohta, Y. and Ichimura, K. (2001). Globosal basal cells are identified as proliferating cells in mouse olfactory epithelium. *Ann. Oto. Rhinol. Laryn.* **110**, 53-55.

Orth, J.M. (1982). Proliferation of Sertoli cells in fetal and postnatal rats: a quantitative autoradiographic study. *Anat. Rec.* **203**, 485-492.

Orth, J.M., Gunsalus, G.L. and Lamperti, A.A. (1988). Evidence from Sertoli cell-depleted rats indicates that spermatid number in adults depends on numbers of Sertoli cells produced during perinatal development. Endocrinology **122**, 787-794.

Pan, D., Dong, J., Zhang, Y. and Gao, X. (2004). Tuberous sclerosis complex: From drosophila to human disease. *Trends Cell Biol.* **14**, 78-85.

Pankov, R. and Yamada, K. M. (2002). Fibronectin at a glance. *J. Cell Sci.* **115**, 3861-3863.

Qian, Y., Liu, S., Guan, Y., Pan, H., Guan, X., Qiu, Z., Li, L., Gao, N., Zhao, Y., Li, X., *et al.* (2013). Lgr4-mediated Wnt/beta-catenin signaling in peritubular myoid cells is essential for spermatogenesis. *Development* **140**, 1751-1761.

Rato, L., Socorro, S., Cavaco, J.E. and Oliveira, P.F. (2010). Tubular fluid secretion in the seminiferous epithelium: ion transporters and aquaporins in Sertoli cells. *J. Membrane Biol*. **236**, 215-224.

Rebourcet, D., Darbey, A., Monteiro, A., Soffientini, U., Tsai, Y. T., Handel, I., Pitetti, J.L., Nef, S., Smith, L.B. and O'Shaughnessy, P.J. (2017). Sertoli cell number defines and predicts germ and leydig cell population sizes in the adult mouse testis. *Endocrinology* **158**, 2955-2969.

Rebourcet, D., O'Shaughnessy, P.J., Monteiro, A., Milne, L., Cruickshanks, L., Jeffrey, N., Guillou, F., Freeman, T.C., Mitchell, R.T. and Smith, L.B. (2014). Sertoli cells maintain Leydig cell number and peritubular myoid cell activity in the adult mouse testis. *PloS One* **9**, e105687.

Richardson, L. L., Kleinman, H. K. and Dym, M. (1995). Basement membrane gene expression by sertoli and peritubular myoid cells in vitro in the rat. *Biol. Reprod.* **52**, 320-330.

Rossi, P., Sette, C., Dolci, S. and Geremia, R. (2000). Role of c-kit in mammalian spermatogenesis. *J. Endocrinol. Invest.* **23**, 609-615.

Sadeghi, S., Reza Talebi, A., Shahedi, A., Reza Moein Md, M. and Abbasi-Sarcheshmeh, A. (2019). Effects of different doses of tamoxifen on the sperm parameters and chromatin quality in mice: An experimental model. *Iran J. Reprod. Med.* **17**, 10.18502/ijrm.v17i4.4553.

Sato, T., Aiyama, Y., Ishii-Inagaki, M., Hara, K., Tsunekawa, N., Harikae, K., Uemura-Kamata, M., Shinomura, M., Zhu, X.B., Maeda, S., *et al.* (2011). Cyclical and patch-like GDNF distribution along the basal surface of sertoli cells in mouse and hamster testes. *PloS One* **6**, e28367.

Schaller, J., Glander, H. J. and Dethloff, J. (1993). Evidence of beta 1 integrins and fibronectin on spermatogenic cells in human testis. *Hum. Reprod.* **8**, 1873-1878.

Schlatt, S., Honaramooz, A., Boiani, M., Scholer, H.R. and Dobrinski, I. (2003). Progeny from sperm obtained after ectopic grafting of neonatal mouse testes. *Biol. Reprod.* **68**, 2331-2335.

Scott, R.W., Arostegui, M., Schweitzer, R., Rossi, F.M.V. and Underhill, T.M. (2019). Hic1 Defines Quiescent Mesenchymal Progenitor Subpopulations with Distinct Functions and Fates in Skeletal Muscle Regeneration. *Cell Stem Cell* **25**, 797-813.

Sebio, A. and Lenz, H. J. (2015). Molecular pathways: Hippo signaling, a critical tumor suppressor. *Clin. Cancer Res.* **21**, 5002-5007.

Setchell, B.P. (1970). The secretion of fluid by the testes of rats, rams and goats with some observations on the effect of age, cryptorchidism and hypophysectomy. *J. Reprod. Fertil.* **23**, 79-85.

Shin, W., Rosin, N.L., Sparks, H., Sinha, S., Rahmani, W., Sharma, N., Workentine, M., Abbasi, S., Labit, E., Stratton, J.A., *et al.* (2020). Dysfunction of Hair Follicle Mesenchymal Progenitors Contributes to Age-Associated Hair Loss. *Dev. Cell* **53,** 185-198.e7.

Shinohara, T., Avarbock, M. R. and Brinster, R. L. (1999). Beta1- and Alpha6-integrin are surface markers on mouse spermatogonial stem cells. *Proc. Natl. Acad. Sci. U. S. A.* **96**, 5504-5509.

Siu, M. K. and Cheng, C. Y. (2008). Extracellular matrix and its role in spermatogenesis. *Adv. Exp. Med. Biol.* **636**, 74-91.

Skalli, O., Ropraz, P., Trzeciak, A., Benzonana, G., Gillessen, D. and Gabbiani, G. (1986). A monoclonal antibody against alpha-smooth muscle actin: A new probe for smooth muscle differentiation. *J. Cell. Biol.* **103**, 2787-2796.

Smith, G. (1962), The effects of ligation of the vasa efferentia and vasectomy on the testicular function in the adult rat. *J. Endocr.* **23**, 385.

Takase, H. M. and Nusse, R. (2016). Paracrine Wnt/beta-catenin signaling mediates proliferation of undifferentiated spermatogonia in the adult mouse testis. *Proc. Natl. Acad. Sci. U. S. A.* **113**, E1489-97.

Takashima, S., Kanatsu-Shinohara, M., Tanaka, T., Morimoto, H., Inoue, K., Ogonuki, N., Jijiwa, M., Takahashi, M., Ogura, A. and Shinohara, T. (2015). Functional differences between GDNF-dependent and FGF2-dependent mouse spermatogonial stem cell self-renewal. *Stem Cell Rep.* **4**, 489-502.

Tsunekawa, N., Nishida, T. and Fujimoto, H. (1999). Expression of the spermatid-specific Hsp70 antigen is conserved in mammals including marsupials. *J. Vet. Sci.* **61**, 381-388.

Turlo, K. A., Scapa, J., Bagher, P., Jones, A. W., Feil, R., Korthuis, R. J., Segal, S.S. and Iruela-Arispe, M.L. (2013). Beta1-integrin is essential for vasoregulation and smooth muscle survival in vivo. *Arterioscler. Thromb. Vasc. Biol.* **33**, 2325-2335.

Valenta, T., Lukas, J., Doubravska, L., Fafilek, B. and Korinek, V. (2006). HIC1 attenuates wnt signaling by recruitment of TCF-4 and beta-catenin to the nuclear bodies. *EMBO J.* **25**, 2326-2337.

Valenzuela-Leon, P. and Dobrinski, I. (2017). Exposure to phthalate esters induces an autophagic response in male germ cells, Environmental epigenetics **3**, dvx010.

Verhoeven, G., Hoeben, E. and De Gendt, K. (2000). Peritubular cell-Sertoli cell interactions: factors involved in PmodS activity. *Andrologia* **32**, 42-45.

Virtanen, I., Kallajoki, M., Narvanen, O., Paranko, J., Thornell, L. E., Miettinen, M. and Lehto, V.P. (1986). Peritubular myoid cells of human and rat testis are smooth muscle cells that contain desmin-type intermediate filaments. *Anat. Rec.* **215**, 10-20.

Walenta, L., Fleck, D., Frohlich, T., von Eysmondt, H., Arnold, G. J., Spehr, J., Schwarzer, J.U., Kohn, F.M., Spehr, M. and Mayerhofer, A. (2018). ATP-mediated events in peritubular cells contribute to sterile testicular inflammation. *Sci. Rep.* ***8***, 1431-018-19624-3.

Wales, M. M., Biel, M. A., el Deiry, W., Nelkin, B. D., Issa, J. P., Cavenee, W. K., Kuerbitz, S.J. and Baylin, S.B. (1995). p53 activates expression of HIC-1, a new candidate tumour suppressor gene on 17p13.3. *Nat. Med.* **1**, 570-577.

Welsh, M., Saunders, P. T., Atanassova, N., Sharpe, R. M. and Smith, L. B. (2009). Androgen action via testicular peritubular myoid cells is essential for male fertility. *FASEB J.* **23**, 4218-4230.

Welsh, M., Sharpe, R. M., Moffat, L., Atanassova, N., Saunders, P. T., Kilter, S., Bergh, A. and Smith, L.B. (2010). Androgen action via testicular arteriole smooth muscle cells is important for leydig cell function, vasomotion and testicular fluid dynamics. *PloS One* **5**, e13632.

Wennerberg, K., Lohikangas, L., Gullberg, D., Pfaff, M., Johansson, S. and Fassler, R. (1996). Beta 1 integrin-dependent and -independent polymerization of fibronectin. *J. Cell Biol.* **132**, 227-238.

Winder, S. J. and Walsh, M. P. (1993). Calponin: Thin filament-linked regulation of smooth muscle contraction. *Cell. Signal.* **5**, 677-686.

Yokonishi, T., McKey, J., Ide, S. and Capel, B. (2020). Sertoli cell ablation and replacement of the spermatogonial niche in mouse, *Nat. Commun.* **11**, 40-019-13879-8.

Yoshida, S., Sukeno, M. and Nabeshima, Y. (2007). A vasculature-associated niche for undifferentiated spermatogonia in the mouse testis. *Science* **317**, 1722-1726.

Yuan, L., Liu, J. G., Zhao, J., Brundell, E., Daneholt, B. and Hoog, C. (2000). The murine SCP3 gene is required for synaptonemal complex assembly, chromosome synapsis, and male fertility. *Mol. Cell* **5**, 73-83.

Zhang, Q., Wang, S. Y., Fleuriel, C., Leprince, D., Rocheleau, J. V., Piston, D. W. and Goodman, R.H. (2007). Metabolic regulation of SIRT1 transcription via a HIC1:CtBP corepressor complex. *Proc. Natl. Acad. Sci. U. S. A.* **104**, 829-833.

Zheng, J., Xiong, D., Sun, X., Wang, J., Hao, M., Ding, T., Xiao, G., Wang, X., Mao, Y., Fu, Y., *et al.* (2012). Signification of hypermethylated in cancer 1 (HIC1) as tumor suppressor gene in tumor progression. *Cancer Microenviron.* **5**, 285-293.

Zheng, K., Wu, X., Kaestner, K. H. and Wang, P. J. (2009). The pluripotency factor LIN28 marks undifferentiated spermatogonia in mouse. *BMC Dev. Biol.* **9**, 38-213X-9-38.

Zhou, X., Zhang, P., Han, H., Lei, H. and Zhang, X. (2019). Hypermethylated in cancer 1 (HIC1) suppresses bladder cancer progression by targeting yes-associated protein (YAP) pathway. *J. Cell. Biochem.* **120**, 6471-6481.

Figures

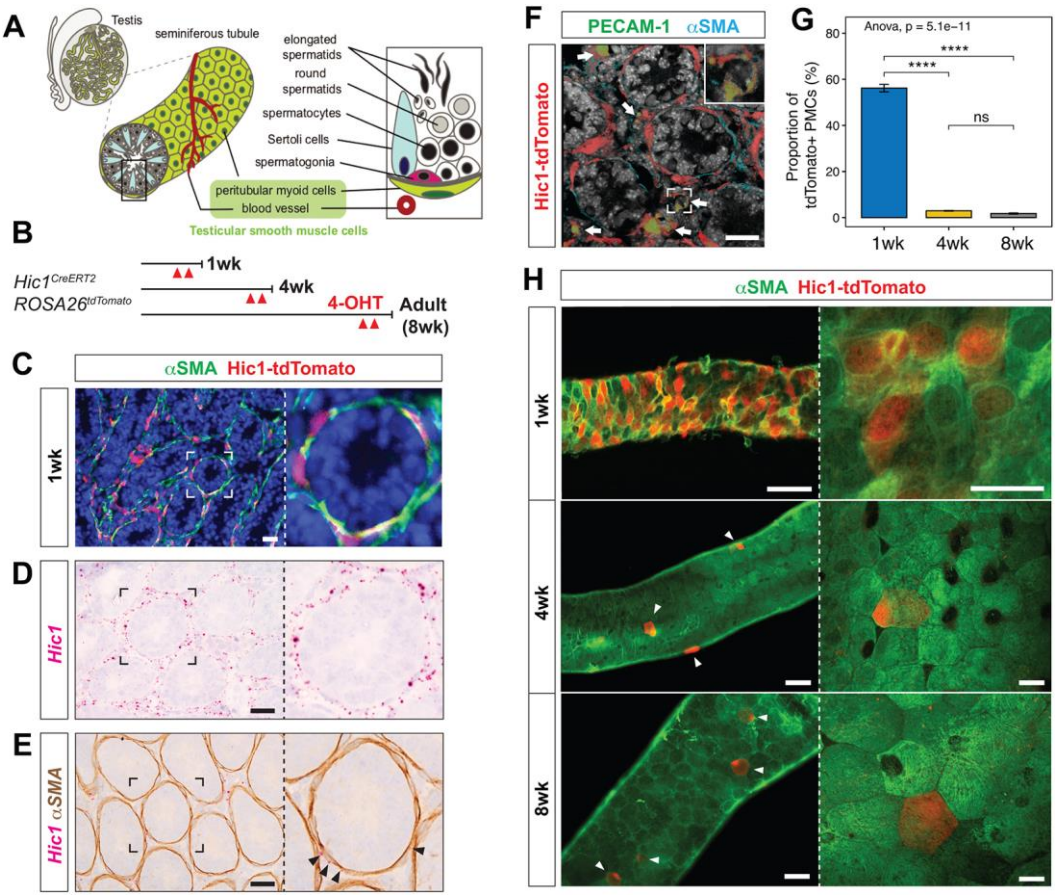

Fig. 1 Identification of *Hic1* expression in mouse testicular smooth muscle cells

(A) Schematic illustration of the anatomy of a mouse testis and seminiferous tubules, highlighting the testicular smooth muscle cells in green. **(B)** Schematic of the experimental strategy to visualize *Hic1* expressing cells with tdTomato. **(C–F)** *Hic1* expression in mouse testicular smooth muscle cells at 1wk-old. **(C)** Anti-αSMA immunohistochemistry (green) and Hic1-tdTomato (red) in testis tissue sections from 1wk-old *Hic1CreER^{T2}:ROSA26^{tdTomato}* mice. **(D, E)** *In situ* hybridization of *Hic1* (red) in 1wk-old mouse testis. *Hic1* signal was observed in the cytoplasm of smooth muscle cells (red in D and E), overlapping with αSMA immunoreactivity (brown in E). **(F)** Hic1-tdTomato in vascular smooth muscle cells distinguished by αSMA (cyan) and adjacent PECAM-1 (green) immunoreactivities. White

arrows indicate vasculature. **(G)** The proportion of Hic1-tdTomato^{+} PMCs at 1wk, 4wk and 8wk-old *Hic1CreER^{T2}:ROSA26^{tdTomato}* mice (n=3 for 1wk, n=4 for 4 and 8wk). Data are shown as mean ± SEM. Analysis was performed using one-way ANOVA followed by Turkey's multiple comparison test. ****P < 0.001. **(H)** Anti-αSMA immunohistochemistry (green) and Hic1-tdTomato (red) in whole-mount seminiferous tubule samples from 1wk, 4wk and 8wk-old *Hic1CreER^{T2}:ROSA26^{tdTomato}* mice. White arrowheads indicate Hic1-tdTomato^{+} PMCs in the panels for 4wk and 8wk. Right panels in C–E and an inset in F show the regions surrounded by broken rectangles at higher magnifications. Right panels in H show the confocal image of PMCs at each age. Bars, 20μm in C–F and right panels in H, 50μm in left panels in H.

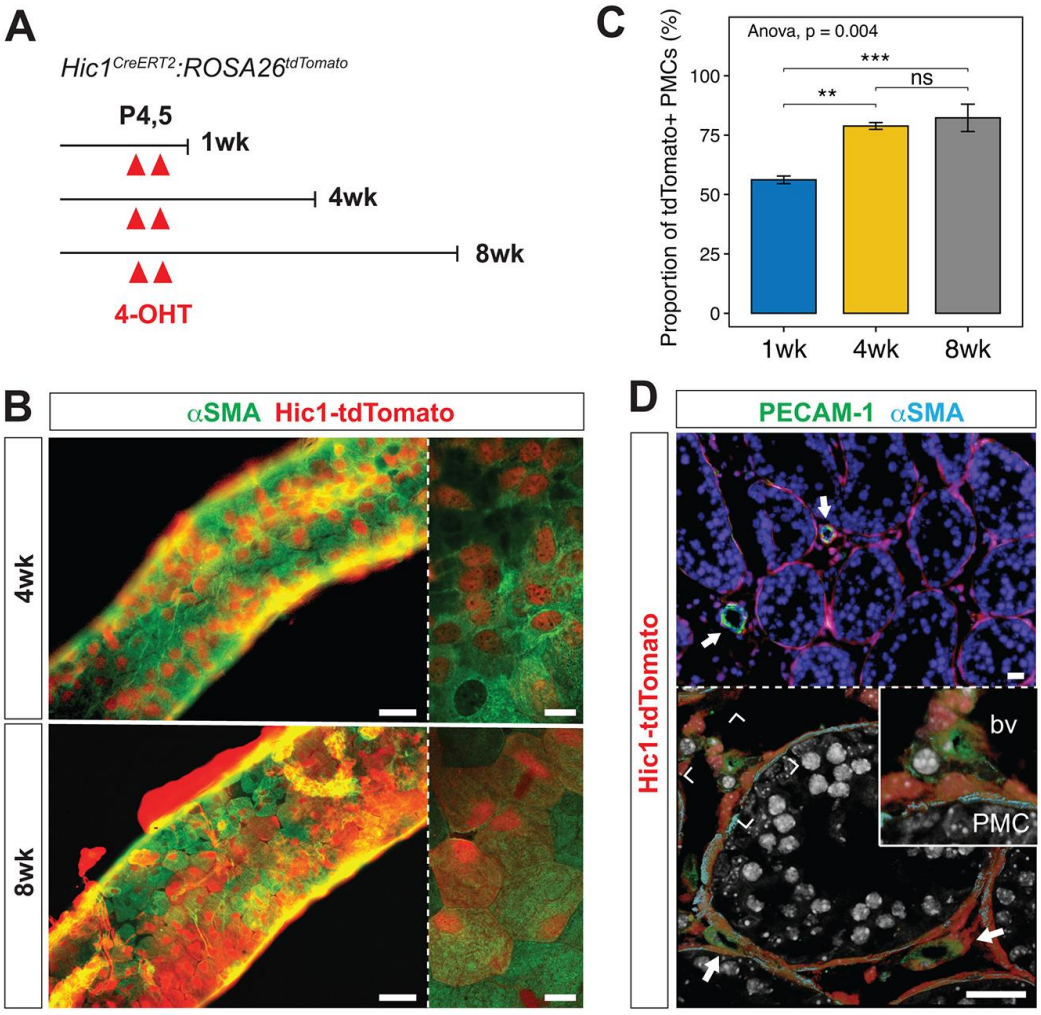

Fig. 2 Adult PMCs and vascular smooth muscle cells arise from *Hic1* expressing cells at 1wk of age

(A) Schematic of the lineage-tracing analysis of cells expressing *Hic1* at 1wk-old. **(B)** Anti-αSMA immunohistochemistry (green) and Hic1-tdTomato (red) in whole-mount seminiferous tubules from 4wk and 8wk-old *Hic1CreER^{T2}:ROSA26^{tdTomato}* mice injected with 4-OHT at P4 and P5. **(C)** The proportion of Hic1-tdTomato^{+} PMCs in 1wk, 4wk and 8wk-old *Hic1CreER^{T2}:ROSA26^{tdTomato}* mice injected with 4-OHT at P4 and P5 (n=3 mice per age). Data are shown as mean ± SEM. Analysis was performed using one-way ANOVA followed

by Turkey's multiple comparison test. **p<0.01, ***p<0.005. **(D)** Hic1-tdTomato in vascular smooth muscle cells distinguished by αSMA (cyan) and adjacent PECAM-1 (green) immunoreactivities in testis tissue sections from 4wk-old *Hic1CreER^{T2}:ROSA26^{tdTomato}* mice. White arrows indicate vasculature in D. Right panels in B show the confocal image of PMCs at each age. An inset in D shows the regions surrounded by broken rectangles at higher magnification. Bars, 50μm in left panels in B and 20μm in D and right panels in B.

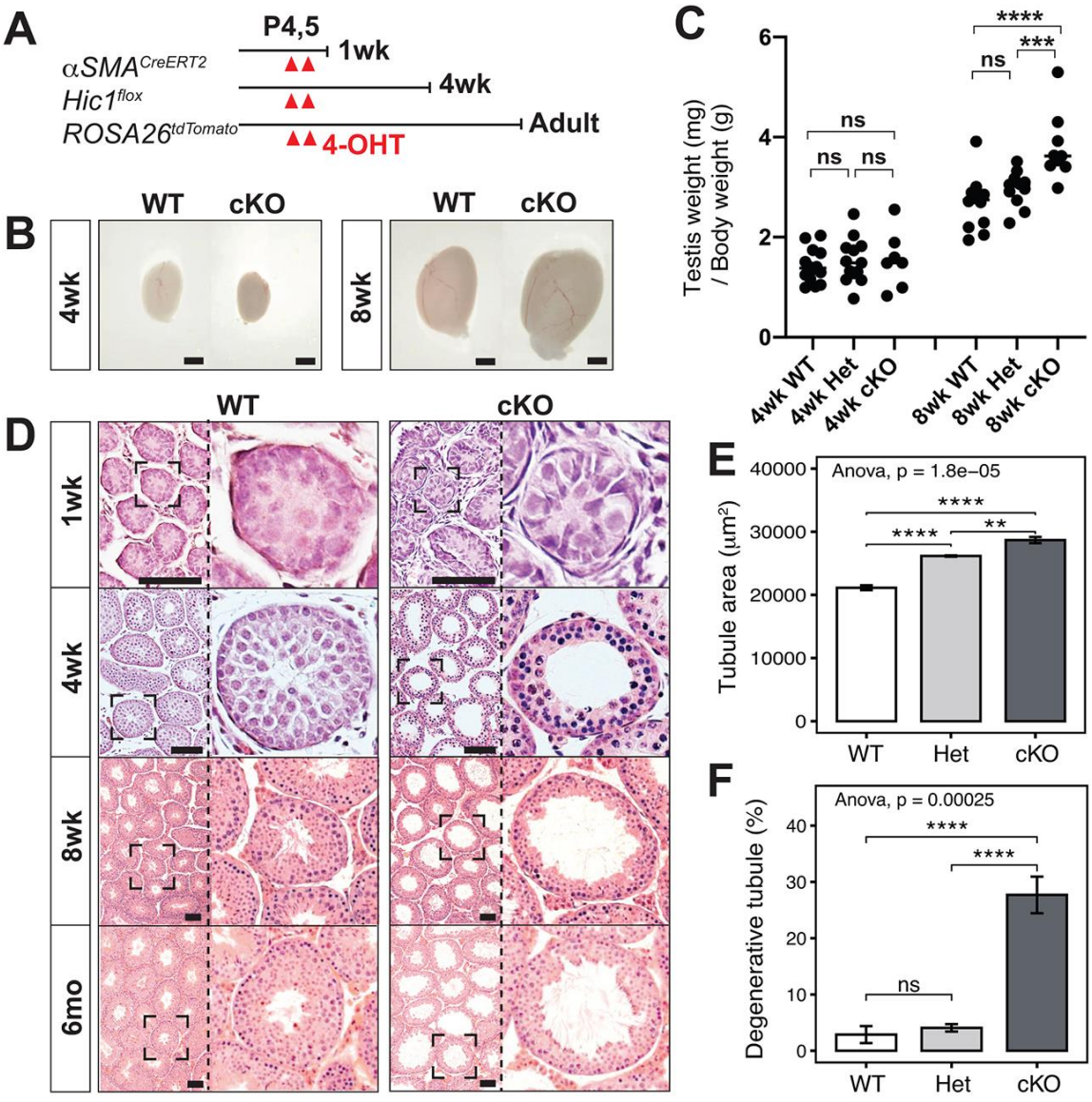

Fig. 3 Testes are larger with tubular dilation in adult *Hic1* cKO mice

(A) Schematic of the experimental strategy to deplete *Hic1* specifically in smooth muscle cells in the postnatal testis. **(B)** Gross morphology of testes from 4wk-old and 8wk-old WT and cKO mice injected with 4-OHT at P4 and P5. **(C)** Relative testis weight to body weight in WT, Het and cKO mice at 4wk and 8wk of age. WT: n=12, Het: n=11, cKO: n=9 in 4wk, WT: n=14, Het: n=13, cKO: n=7 in 8wk. **(D)** Histology of the testes from WT and cKO mice at 1wk, 4wk, 8wk and 6mo of age. Right panels show the regions surrounded by broken

rectangles in left panels at higher magnifications. **(E)** Average area of seminiferous tubule cross sections and **(F)** the percentage of degenerative seminiferous tubule cross sections in WT, Het and cKO mice at 8wk of age. n=3 for each genotype. Data are shown as mean ± SEM. Analysis was performed using one-way ANOVA followed by Turkey's multiple comparison test. **p<0.01, ***p<0.005, ****p<0.001. Bars, 1mm in B, 200μm in D.

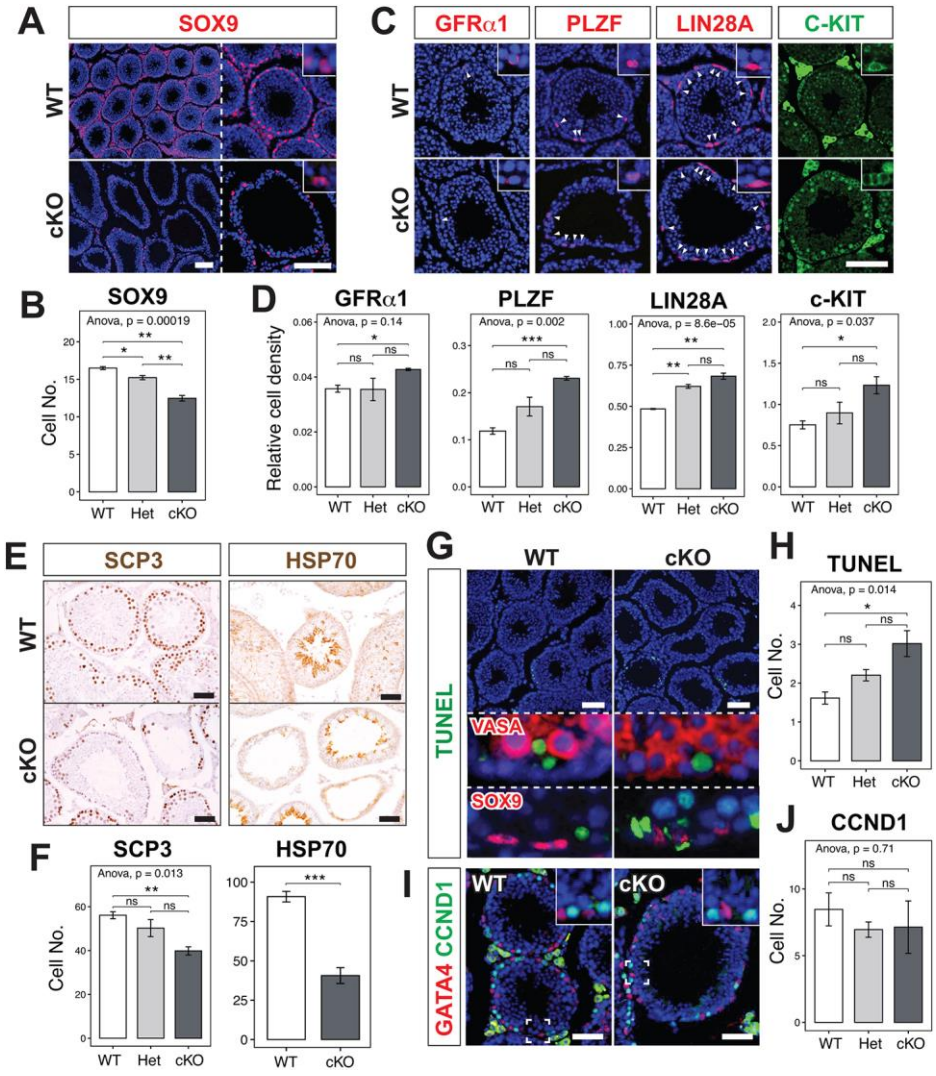

Fig. 4 Distribution of Sertoli cells and germ cells in cKO mice

(A–F) Distribution of Sertoli cells (A–B) and germ cells (C–F) within the seminiferous tubule from 8wk-old WT and cKO mice. **(A–B)** The number of Sertoli cells marked with SOX9 immunoreactity (red in A) per cross-sectioned seminiferous tubule was significantly decreased in cKO mice. **(C–D)** Relative cell density of spermatogonia positive for GFRα1, PLZF, LIN28A and c-KIT (red or green in C) compared to the number of $SOX9^{+}$ Sertoli cells (A) were significantly larger in cKO mice compared to WT mice. **(E–F)** The numbers of cells positive for SCP3 and HSP70 (brown in E) per cross-sectioned seminiferous tubules were significantly smaller in cKO mice. **(G)** TUNEL-stained (green) testis section with anti-

VASA or SOX9 immunohistochemistry (red in lower two panels) from WT and cKO mice at 8wk of age. **(H)** The number of $TUNEL^+$ apoptotic cells per cross-sectioned seminiferous tubule were larger in cKO mice. **(I–J)** The number of $CCND1^+$ proliferative cells (red in I) negative for GATA4 immunoreactivity (green in I) per seminiferous tubule cross section were not significantly different between WT and cKO mice. In this analysis, we used paraffin-embedded samples to conserve the morphology of the samples, in which endogenous tdTomato in the mouse model were diminished and unobservable. n=3 for each genotype. Data are shown as mean ± SEM. Analysis was performed using one-way ANOVA followed by Turkey's multiple comparison test or student's t-test. Small insets in A and C show magnification of the cells positive for each marker. Insets in I show the magnification of regions surrounded by broken rectangles. White arrowheads in C indicate the cells positive for each marker. *P<0.05, **P<0.01, ***P<0.005 and ****P<0.001. Bars, 50μm.

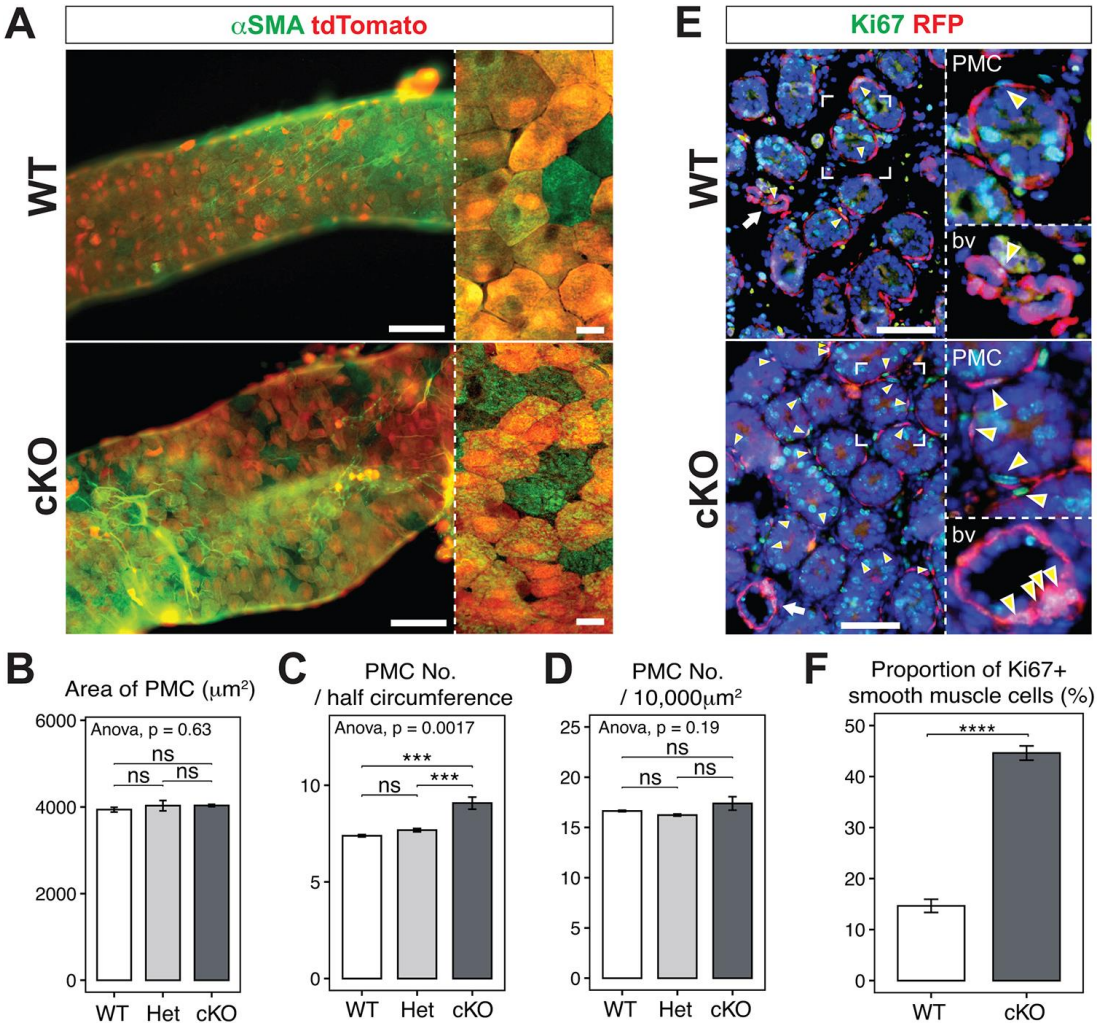

Fig. 5 Size and density of PMCs were not different in WT and cKO mice, yet the number of PMCs was increased in cKO mice

(A) Anti-αSMA immunohistochemistry (green) and tdTomato (red) in whole-mount seminiferous tubules from WT and cKO mice at 8wk-old. **(B)** Average surface area of the seminiferous tubules covered by a single PMC in WT, Het and cKO mice. **(C)** Number of PMCs per half circumference of seminiferous tubule in WT, Het and cKO mice. **(D)** Density of PMCs on the surface area of seminiferous tubules, shown as the number of PMCs per area of 10000μm^2. n=3 for each genotype. **(E)** Anti-Ki67 immunohistochemistry (green) and RFP

signal (red) in cryosections from WT and cKO mice at 1wk-old. **(F)** The proportion of $Ki67^{+}$ proliferative smooth muscle cells was higher in cKO mice compared with WT mice. In this analysis, we visualized tdTomato with RFP immunoreactivity due to the permeabilization process required for Ki67 staining, which diminishes the endogenous tdTomato. Data are shown as mean ± SEM. Analysis was performed using one-way ANOVA followed by Turkey's multiple comparison test (B–D) or student's t-test (F). *** $p<0.005$, **** $p<0.001$. Right panels in A show the confocal image of PMCs from each genotype. In E, right upper panels labelled "PMC" show the magnification of the regions surrounded by broken rectangles, while right lower panels labelled "bv" show the magnified image of the blood vessels indicated with white arrows. Yellow arrowheads in E indicate smooth muscle cells positive for both Ki67 and RFP. Bars, 100μm in left panels in A, 20μm in right panels in A and 50μm in E.

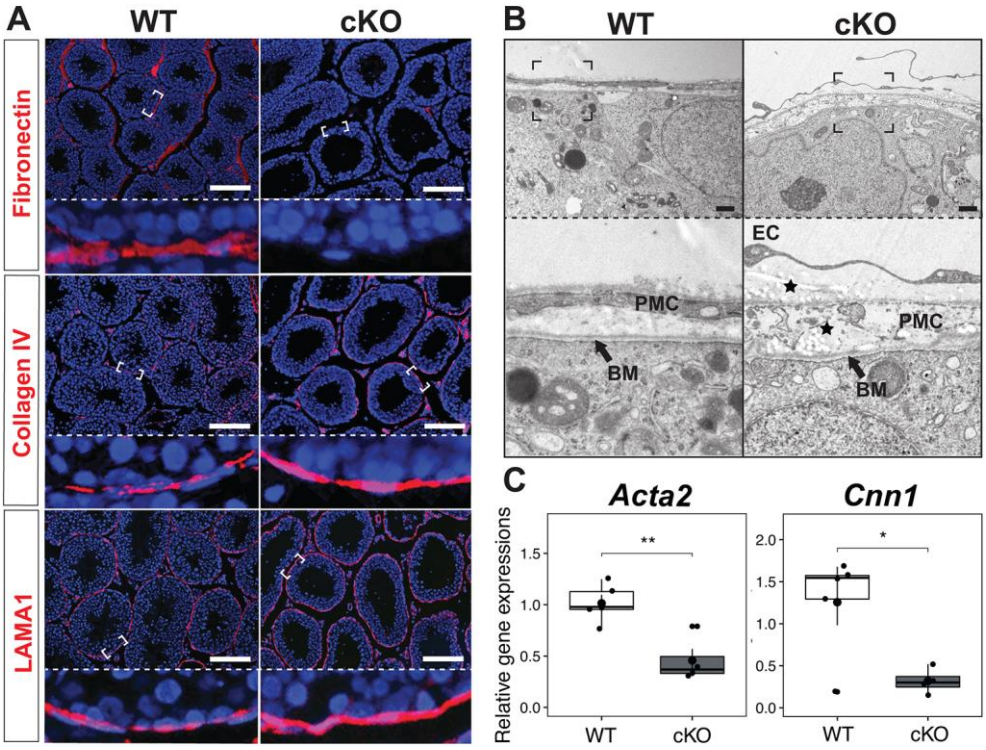

Fig. 6 *Hic1* deletion in testicular smooth muscle cells affects their morphology and functionality

(A) Immunohistochemistry of ECM proteins (red) in testis tissue sections from 8wk-old WT and cKO mice, showing hardly any fibronectin signal with relatively strong collagen IV and LAMA1 signal in the basement membrane in cKO testes. **(B)** Transmission electron micrographs of 8wk-old WT and cKO mouse testes, visualizing the ultrastructure of PMCs together with the basement membrane in 8wk-old WT and cKO testis. BM: basement membrane, EC: endothelial cell. Stars indicate the accumulated lipid-like structures around the basement membrane. **(C)** Gene expression levels of *Acta2* and *Cnn1* in tdTomato^{+} cells sorted from 8wk-old WT and cKO mice. n=4 for WT, n=5 for cKO. Lower panels in A and B show the magnification of regions surrounded by broken rectangles, respectively. Analysis was performed using student's t-test. *$p<0.05$, **$p<0.01$. Bars, 100μm in A and 500nm in B.

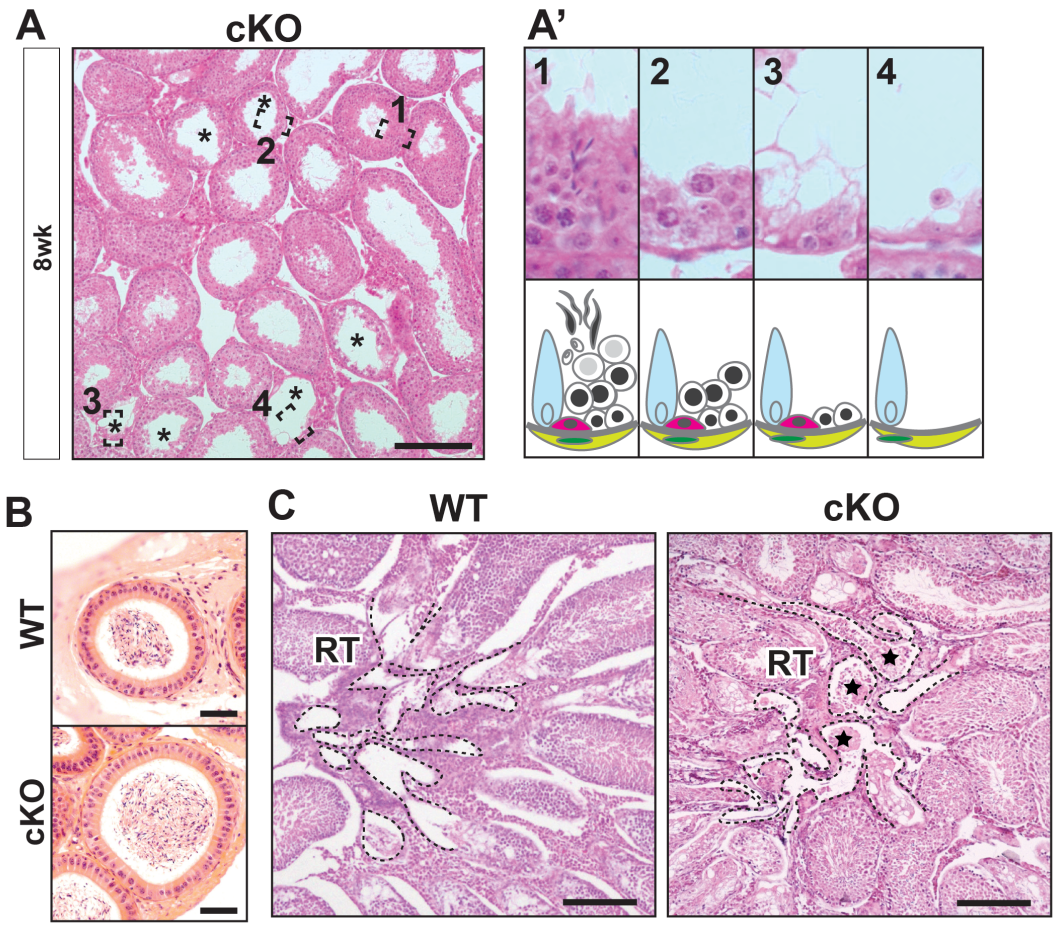

Fig. S1 Degeneration and dilation of seminiferous tubulesin cKO is independent from ER expression

(A) Histology of the testis from 8wk-old cKO mouse. Right panels A'1–4 show the regions surrounded by broken rectangles 1–4 in the left panel at higher magnifications together with schematic illustrations below. * indicates degenerative tubules in A. **(B)** Histology of the epididymis from adult WT and cKO mice. **(C)** Histology of the rete testis (RT, region outlined by broken line) in 8wk-old WT and cKO mouse. Stars represent the cell debris observed in the luminal region of RT in cKO testis. Bars, 50μm in B, 200μm in A and C.

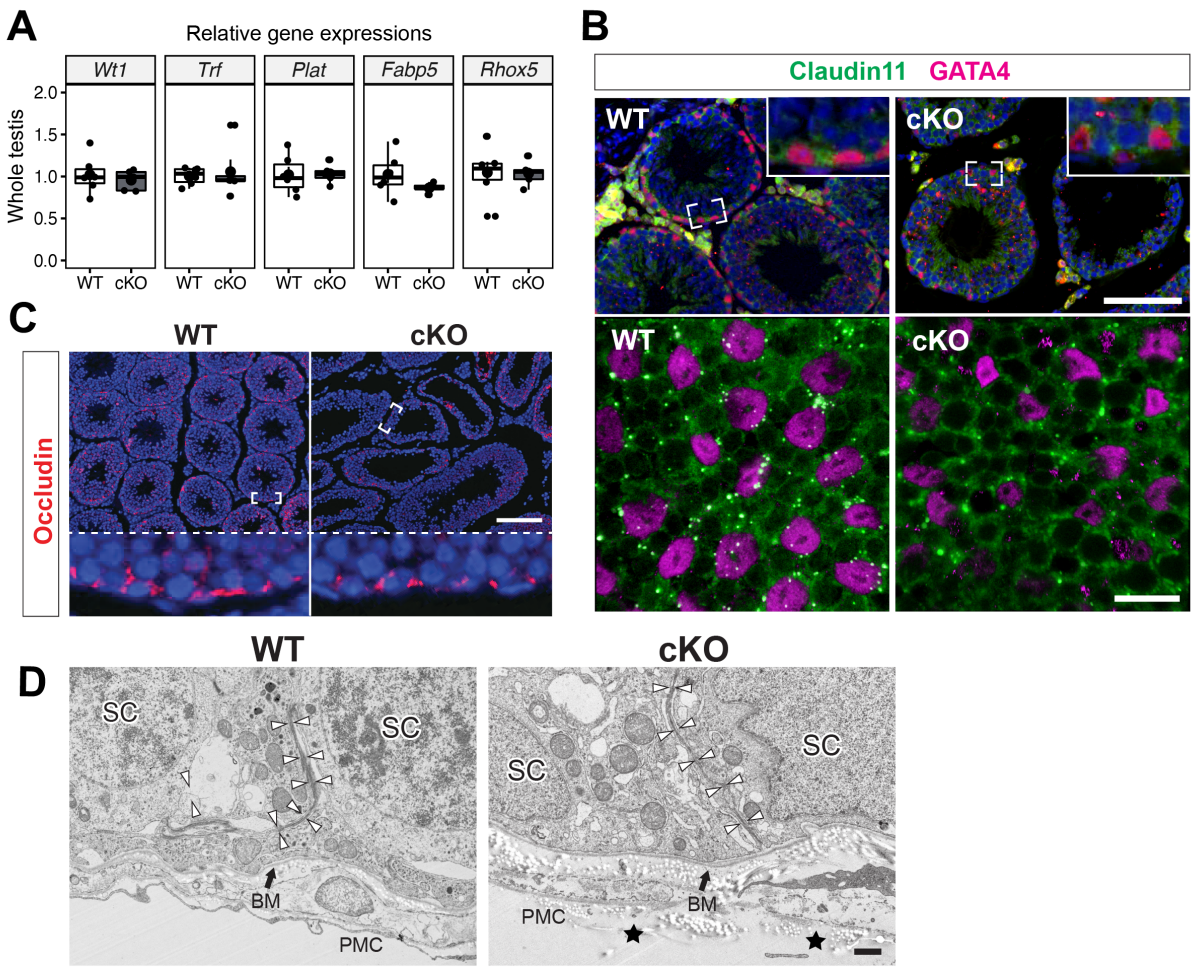

Fig. S2 Sertoli cell functionwas not affected in cKO mice

(A) Expression levels of genes related to Sertoli cell function in whole testis of 8wk-old WT and cKO mice (n=6 for WT, n=5 for cKO). **(B–D)** Blood-testis barrier (BTB) appeared to be unaffected in cKO mice. (B) Anti-Claudin 11 (green) and GATA4 (red) immunohistochemistry in testis section (upper panels) and whole-mount seminiferous tubules (lower panels) from WT and cKO mice at 8wk-old. Claudin 11 signals were observed around the GATA4-postive Sertoli cell nuclei. (C) Anti-Occludin (red) immunohistochemistry in testis section from WT and cKO mice at 8wk-old. Lower panels in C show the magnification of regions surrounded by broken rectangles. (D) Transmission electron micrographs of 8wk-old WT and cKO mouse testes, visualizing similar ultrastructure of tight junctions between Sertoli cells in WT and cKO testis. White arrowheads point to intact junctions between Sertoli cells. BM: basement membrane, SC: Sertoli cell. Stars indicate accumulated lipid-like structures around the basement membrane. Bars, 100μm in upper panels in B and C, 20μm in lower panels in B and 1μm in D.

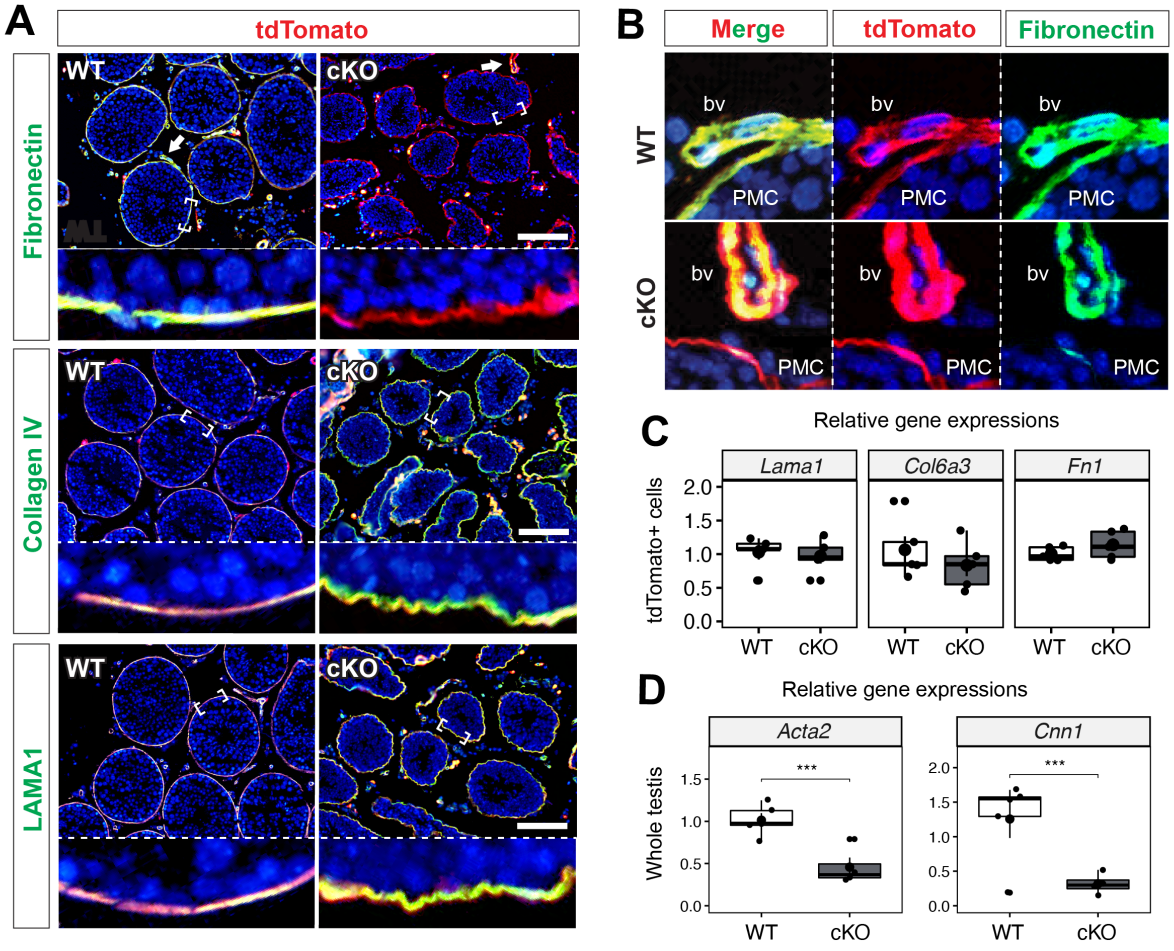

Fig. S3 Fibronectin is present in vascular smooth musclecells, but not in PMCs of cKO mice

(A, B) Cryosections of 8wk-old WT and cKO mouse testes, showing the immunoreactivity of ECM proteins (green) and tdTomato signals (red). Lower panels in A show magnification of the region surrounded by broken rectangles in upper panels. Bars, 100μm. (B) Higher magnification of the region indicated with white arrow in the top panels in A. In cKO testes, fibronectin signals were observed intensely in vascular smooth muscle cells but not in PMCs. bv: blood vessel. **(C)** Expression levels of genes encoding ECM proteins in tdTomato^{+} cells sorted from 8wk-old WT and cKO mice. (n=5 for each genotype). **(D)** Expression levels of genes encoding smooth muscle contractile proteins in whole testis from 8wk-old WT and cKO mice. (n=6 for WT, n=5 for cKO). ***p<0.005. Analysis was performed using student's t-test. Bars, 100μm.

Supplementary Tables

Table S1. List of antibodies used in this study

Antigen	Dilution	Description	Company	CAT#
αSMA	1/500 IHC, 1/1,000 WB	Mouse monoclonal	Sigma	A5228
c-KIT	1/200 IHC	Goat polyclonal	R&D systems	AF1356
Claudin 11	1/100 IHC	Rabbit polyclonal	Thermo Fisher	36-4500
CNN1	1/5000 WB	Rabbit monoclonal	Abcam	ab46794
CNND1	1/400 IHC	Rabbit monoclonal	Abcam	ab16663
Collagen IV	1/100 IHC	Rabbit polyclonal	Abcam	ab6586
Fibronectin	1/100 IHC	Rabbit polyclonal	Abcam	ab2413
GATA4	1/100 IHC	Goat polyclonal	Santa cruz	sc1237
GFRα1	1/100 IHC	Goat polyclonal	R&D systems	AF560
HSP70	1/1000 IHC	Rabbit polyclonal	Abcam	ab79852
HPRT1	1/20,000 WB	Rabbit polyclonal	Thermo Fisher	A305-306A
Ki67	1/100 IHC	Mouse monoclonal	Leica	NCL-L-Ki67-MM1
Laminin	1/200 IHC	Rabbit polyclonal	Abcam	ab26300
LIN28A	1/200 IHC	Rabbit monoclonal	Cell Signaling	8706
PECAM-1	1/100 IHC	Rat monoclonal	BD Pharmingen	550274
PLZF	1/100 IHC	Rabbit polyclonal	Santa cruz	sc22889
RFP	1/200 IHC	Rabbit polyclonal	MBL	PM005
SCP3	1/500 IHC	Mouse monoclonal	Santa cruz	sc74569
SOX9	1/100 IHC	Rabbit polyclonal	Milipore	AB5535
VASA	1/1000 IHC	Rabbit polyclonal	Abcam	ab13840

Table S2. List of primers used for qPCR

Target gene	Direction	Sequence (5' → 3')
Acta2	F	TGCTGTCCCTCTATGCCTCT
	R	GAAGGAATAGCCACGCTCAG
Col6a3	F	GGAACCACGGAAGAGAGCAA
	R	CAGGGAACTGACCCAAGACA
Cnn1	F	CAAGCTGGCCCAGAAATACGACC
	R	TCTTCACAGAACCCGGCTGCAG
Esr1	F	TTGAACCAGCAGGGTGGC
	R	AGGCTTTGGTGTGAAGGGTC
Esr2	F	GGCAAGCTCATCTTTGCTCC
	R	CTCATCCCTTGGGACAGCAC
Fabp5	F	CGGTCAAAACCGAGAGCACA
	R	GTGCAGACCGTCTCAGTTTTTC
Fn1	F	GCCACCATTACTGGTCTGGA
	R	ACCAGTTGGGGAAGCTCATC
Hprt	F	AGCAGTACAGCCCCAAAATGGT
	R	CCAACAAAGTCTGGCCTGTATCC
Lama1	F	TATCCTGCCCACATCAAACAG
	R	CTTGTAGGTCAAAGGCTCGG
Plat	F	AGATGAGCCAACGCAGACAA
	R	CTTGGTTCGCTGCAACTTCG
Rhox5	F	GCAGCGCACTAATTCCTTTG
	R	GCAGCCCTCCTGATCTTAAA
Trf	F	CGTAGGCGCATTCAAGTGTC
	R	ATTGGTCCCTGTCAGCCTTC
Wt1	F	CCAGTGTAAAACTTGTCAGCGAAA
	R	ATGAGTCCTGGTGTGGGTCTTC

Supplementary Movies

Movie 1. Active contraction of adult WT seminiferous tubule

Movie 2. Contraction of adult cKO seminiferous tubule

Supplementary Materials and Methods

Western blot

Testes collected from 8wk-old WT and cKO mice were rinsed with PBS and homogenized in cold RIPA buffer containing protease inhibitor cocktail (Sigma). Protein concentration was determined by a DC protein assay (Bio-Rad). Equal amounts of total protein from each sample were then mixed with SDS loading buffer and boiled at 95ºC for 10 minutes. The target proteins were separated by SDS-PAGE, then transferred onto PVDF membranes. The membranes were blocked with 5% BSA/TBST with 0.1% Tween 20, and then incubated with primary antibodies listed in Table 1 at 4°C overnight. The membranes were washed with 0.1% Tween 20/TBST and incubated with secondary antibodies for at least 1 hour at room temperature. All secondary antibodies were diluted into 5% non-fat milk in 1X TBST with 0.1% Tween 20. The membranes were washed with 0.1% Tween 20/TBST. ECL was carried out with Pierce™ ECL 2 Western Blotting Substrate (Thermo Fisher) and the signals were visualized with ChemiDoc™ XRS+ system (Bio-Rad). The expression of HPRT1 was used as an internal control in this experiment.

Efferent duct ligation

Mice were anesthetized with isoflurane, and the efferent duct of a testis was ligated under a dissecting microscope as reported previously (Smith, 1962) with 7-0 nylon suture. Contralateral testis from the same animal was kept as a control without ligation. Mice were euthanized 1 week after the ligation, and their testes were collected, weighed, dispersed into seminiferous tubule fragments and analyzed by αSMA immunohistochemistry in whole-mount preparation. Weight of the ligated testis was 1.30 ± 0.04 times heavier than the control testis at 1 week after the ligation ($p=0.034$, student's t-test, $n=3$). More than 30 whole-mount seminiferous tubules were analyzed per animal for the quantification of PMC number/half circumference of seminiferous tubules.